NBSIR 73-281

AFOSR SCIENTIFIC REPORT
AFOSR-TR-74-0063

Thermodynamics of Chemical Species Important to Rocket Technology

Various authors

Physical Chemistry Division
Institute for Materials Research
National Bureau of Standards
Washington, D. C. 20234

NBSIR 73-281

AFOSR SCIENTIFIC REPORT
AFOSR-TR-74-0063

THERMODYNAMICS OF CHEMICAL SPECIES
IMPORTANT TO ROCKET TECHNOLOGY

Various authors

Physical Chemistry Division
Institute for Materials Research
National Bureau of Standards
Washington, D. C. 20234

FOREWORD

Structure, propulsion, and guidance of new or improved weapons delivery systems are dependent in crucial areas of design on the availability of accurate thermodynamic data. Data on high-temperature materials, new rocket propellant ingredients, and combustion products (including exhaust ions) are, in many cases, lacking or unreliable. A broad integrated research program at the National Bureau of Standards has supplied new or more reliable thermodynamic properties essential in several major phases of current propulsion development and application. Measured were compounds of those several chemical elements important in efficient propulsion fuels; those substances most affecting ion concentrations in such advanced propulsion concepts as ion propulsion; and the transition and other refractory metals (and their pertinent compounds) which may be suitable as construction materials for rocket motors, rocket nozzles, and nose cones that will be durable under extreme conditions of high temperature and corrosive environment. The properties determined extend in temperature up to 6000 degrees Kelvin. The principal research activities were experimental, and involved developing new measurement techniques and apparatus, as well as measuring heats of reaction, of fusion, and of vaporization; specific heats; equilibria involving gases; several properties from fast processes at very high temperatures; spectra of the infrared, matrix-isolation, microwave, and electronic types; and mass spectra. Some of these techniques, by relating thermodynamic properties to molecular or crystal structures, make it possible to tabulate reliably these properties over far wider ranges of temperature and pressure than those actually employed in the basic investigations. Additional research activities of the program have involved the critical review of published chemical-thermodynamic (and some chemical-kinetic) data, and the generation of new thermochemical tables important in current chemical-laser research.
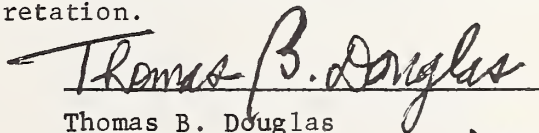
i

Previous reports describing related work have the NBS Report Nos.
6297, 6484, 6645, 6928, 7093, 7192, 7437, 7587, 7796, 8033, 8186,
8504, 8628, 8919, 9028, 9389, 9500, 9601, 9803, 9905, 10004, 10074,
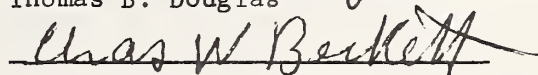10326, 10481, 10904, and NBSIR 73-280.

ABSTRACT

This report (covering January-June 1973) constitutes the Final Report on all past phases of the program except that measuring thermophysical properties by high-speed techniques, which is continuing. The nature and scope of the subjects covered in this report may be inferred from the detailed Table of Contents to be found on the following pages.

Using a subsecond-duration transient technique, the specific heat, electrical resistivity, and hemispherical total emittance were simultaneously measured over the temperature range 1500-2800 K for iron (99.9 + % pure) and for the alloy 80 Nb-10 Ta-10 W (nominal composition by weight), with estimated uncertainties of 3%, 0.5-1%, and 3%, respectively. The specific heats found for the alloy are about 2.5% above the additive (Kopp's law) values; the electrical resistivity shows significant departure from Matthiesen's law, the resistivity-temperature curve showing (like pure Nb) negative departure from linearity. The specific heat and electrical resistivity of iron both increase during the gamma-to-delta transformation (1673 and 1683 K on two specimens, with an estimated heat of transformation of 890 J mol^{-1}). The work on iron demonstrates the feasibility of applying a rapid-pulse heating technique to solid-solid transformations. The following melting points (and normal spectral emittance for 650 nm at the melting point) were found: Fe, 1808 ±5K (0.355); 99Nb-1 Zr, 2737 ±10 K (0.351); 80 Nb-10 Ta- 10 W, 2814 ±10 K (0.333); 90 Ta-10 W, 3286 ±15 K (0.396).

Preliminary values are reported for the first time for the standard heat of formation and a vapor pressure of the subfluoride of molybdenum MoF_5. Solution calorimetry, involving a series of steps including oxidation by XeO_3 in aqueous HF, yielded, at 298 K, ΔH_f° [$MoF_5(c)$] = -1395.74 ± 4.6 kJ mol^{-1} (-333.59 ± 1.1 kcal mol^{-1}), with a maximum uncertainty of about 17 kJ mol^{-1} (4 kcal mol^{-1}) in ΔH_f [$MoF_6(\ell)$] - ΔH_f° [$MoF_5(c)$]; final results will include some minor heats of dilution. (Earlier solution calorimetry involving alkaline solutions of XeO_3 was unsatisfactory owing to spontaneous decomposition of the XeO_3.) A new static method for measuring small vapor pressures has reproduced known values for I_2 and MoF_6 to within 1%. In extending the method to MoF_5, it was found that the MoF_6 (added to suppress sample disproportionation) could be accounted for reliably only after crystallizing the MoF_5. The vapor pressure of MoF_5 (ℓ) thus measured at 393 K, when compared with the earlier transpiration result for this temperature, indicates that the saturated vapor contains about 85 or 90 mole % of the monomer species, depending on the method of interpretation.

Thomas B. Douglas

Charles W. Beckett

TABLE OF CONTENTS

TABLE OF CONTENTS (Continued)

Chapter 1

SIMULTANEOUS MEASUREMENTS OF SPECIFIC HEAT,

ELECTRICAL RESISTIVITY AND HEMISPHERICAL

TOTAL EMITTANCE OF THE TERNARY ALLOY

NIOBIUM (80) - TANTALUM (10) - TUNGSTEN (10)

IN THE RANGE 1500 TO 2800 K[*]

Ared Cezairliyan
National Bureau of Standards
Washington, D. C.   20234

Abstract

Simultaneous measurements of the specific heat, electrical
resistivity, and hemispherical total emittance of the ternary alloy
niobium-tantalum-tungsten (nominal composition, 80-10-10 percent
by weight) in the temperature range 1500 to 2800 K by a subsecond-
duration, transient technique are described. Estimated inaccuracies
of measured properties are: 3% for specific heat and hemispherical
total emittance, and 0.5% for electrical resistivity. Properties
of the alloy are compared with the properties of the constituent
elements. The values of measured specific heat are approximately
2.6% (on the average) higher than the values computed according
to Kopp's additivity law. However, this difference is within the
combined estimated errors. The electrical resistivity results
indicate a significant departure from Matthiessen's law. Like the
major constituent niobium, the alloy showed a negative departure from
linearity in the curve of electrical resistivity versus temperature.

---

1. Introduction

In this paper, application of a transient technique to the simultaneous measurements of specific heat, electrical resistivity, and hemispherical total emittance of the ternary alloy niobium-tantalum-tungsten (nominal composition 80-10-10 percent by weight) in the temperature range from 1500 to 2800 K is described.

The method is based on rapid resistive self-heating of the specimen from room temperature to high temperatures (above 1500 K) in less than one second by the passage of an electrical current pulse through it; and on measuring, with millisecond resolution, such experimental quantities as current through the specimen, potential drop across the specimen, and specimen temperature. Details regarding the construction and operation of the measurement system, the methods of measuring experimental quantities, and other pertinent information, such as the formulation of relations for properties, etc. are given in earlier publications [1, 2][1].

2. Measurements

Specimen   The specimen was a tube fabricated from a rod[2] by removing the center portion by an electro-erosion technique. The nominal dimensions of the specimen were: length, 102 mm; outside diameter, 6.3 mm; and wall thickness, 0.5 mm. The outer surface of the specimen was polished to reduce heat loss due to thermal radiation.

---

[1]Figures in brackets indicate the literature references at the end of this paper.

[2]The specimen in rod form was furnished by the Fansteel Metals Corporation.

According to the manufacturer's analysis, the composition
(by weight) of the major constituents of the specimen was: niobium,
81%; tantalum, 9.7%; and tungsten, 9.3%. The impurities (in ppm)
were: hafnium, molybdenum, silicon and zirconium, 100 each; iron
and titanium, 50 each; C, 11; 0, 51; N, 44; and H, 5.

Procedure: The measurements were performed in the temperature
interval 1500 to 2800 K. To optimize the operation of the pyrometer,
this interval was divided into six ranges. One experiment was
performed in each range. Before the start of the experiments, the
specimen was heat treated by subjecting it to 30 heating pulses
(up to approximately 2200 K). All the experiments were conducted
with the specimen in a vacuum environment of approximately 10^{-5}
torr. To optimize the operation of the measurement system, the
heating rate of the specimens was varied depending on the desired
temperature range by adjusting the value of a resistance in series
with the specimen. Duration of current pulses in the experiments
ranged from 430 to 500 ms; and the heating rate ranged from 3500
to 5000 K s^{-1}. Radiative heat loss from the specimen amounted to
approximately 1% at 1500 K, and 14% at 2800 K of the input power.

3. Experimental Results

The properties reported in this paper are based on the
International Practical Temperature Scale of 1968 [3]. In all
.computations, the geometrical quantities are based on their room
temperature (298 K) dimensions. The experimental results for
properties are represented by polynomial functions in temperature
obtained by least squares approximation of the individual points.
The final values of properties at 100 degree temperature intervals
computed using the functions are presented in Table 1. Results
obtained from individual experiments are given in the Appendix
(Tables A-1 and A-2). Each number tabulated in these tables
represents results from over fifty original data points.

Specific Heat. Specific heat was computed from data taken
during the heating period. A correction for power loss due to
thermal radiation was made using the results on hemispherical total
emittance. The function for specific heat (standard deviation =
0.4%) that represents the results in the temperature range 1500 to
2800 K is:

$$c_p = -0.1042 + 5.889 \times 10^{-4}T - 3.019 \times 10^{-7}T^2 + 5.758 \times 10^{-11}T^3 \qquad (1)$$

where T is in K, and c_p is in J $g^{-1}K^{-1}$. The deviations of the
experimental results from equation (1) are shown on figure (1).

Table 1

Specific heat, electrical resistivity, and hemispherical total

emittance of the ternary alloy niobium (80) - tantalum (10)- tungsten (10)

Temp. K	c_p J g^{-1}K^{-1}	ρ[a] $10^{-8}\Omega$ m	ϵ[a]
1500	0.2942	57.27	
1600	0.3010	60.02	
1700	0.3073	62.74	0.217
1800	0.3135	65.43	0.227
1900	0.3198	68.10	0.237
2000	0.3266	70.74	0.246
2100	0.3344	73.36	0.255
2200	0.3433	75.95	0.264
2300	0.3538	78.51	0.272
2400	0.3662	81.05	0.280
2500	0.3809	83.55	0.287
2600	0.3981	86.04	0.294
2700	0.4183	88.49	
2800	0.4418	90.92	

[a]Based on ambient temperature (298 K) dimensions.
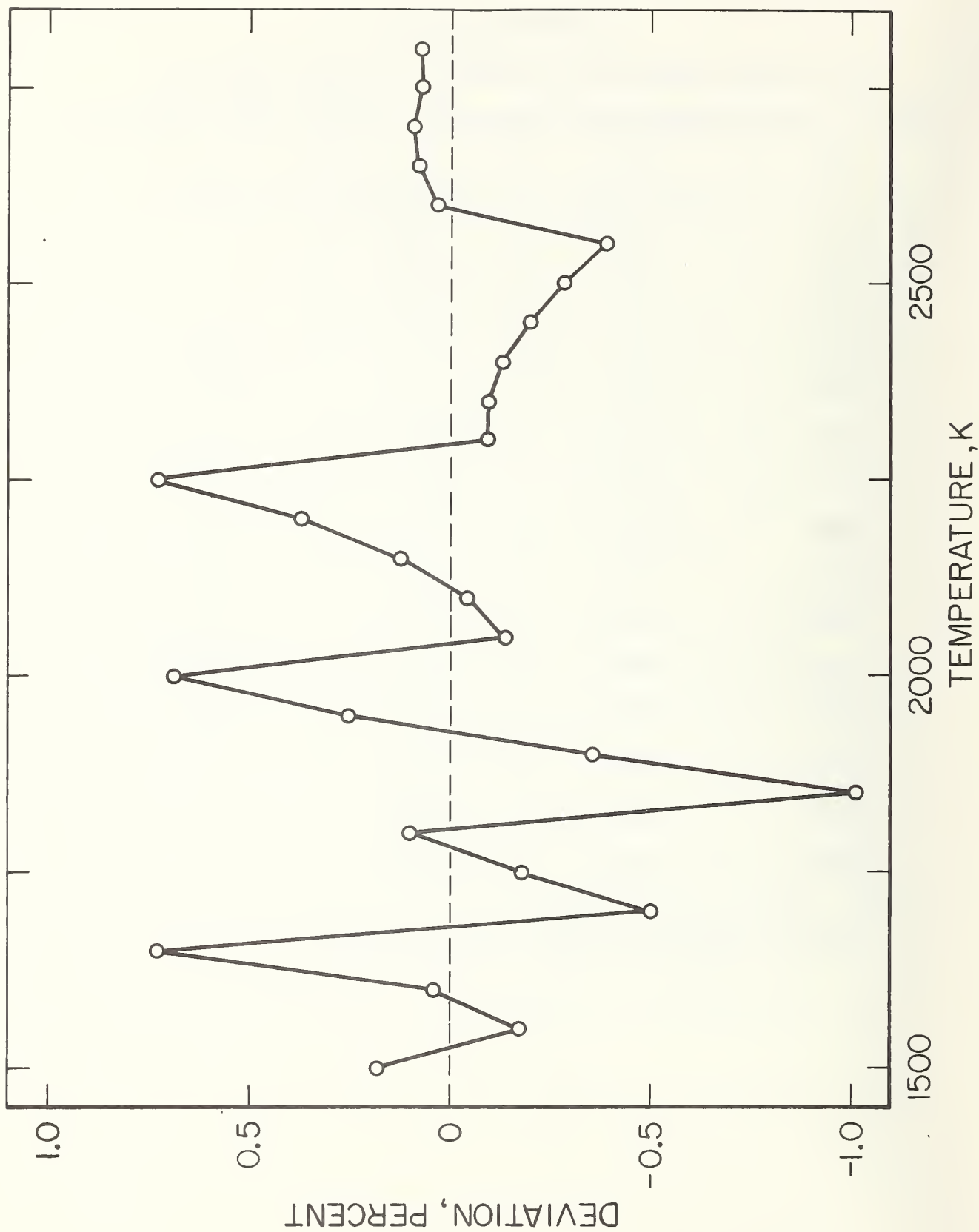
FIGURE 1.   Deviation of specific heat results from equation (1).

Electrical Resistivity: The electrical resistivity was determined from the same experiments that were used to calculate the specific heat. The function for electrical resistivity (standard deviation = 0.03%) that represents the results in the temperature range 1500 to 2800 K is:

$$\rho = 12.86 + 3.160 \times 10^{-2}T - 1.329 \times 10^{-6}T^2 \tag{2}$$

where T is in K, and ρ is in 10^{-8} Ω m. The deviations of the experimental results from equation (2) are shown on figure 2. The measurement, before the pulse experiments, of the electrical resistivity of the specimen at 293 K with a Kelvin bridge yielded a value of 17.2×10^{-8} Ω m.

Hemispherical Total Emittance: Hemispherical total emittance was computed using data taken during both heating and initial free radiative cooling periods. The function for hemispherical total emittance (standard deviation = 0.6%) that represents the results in the temperature range 1700 to 2600 K is:

$$\epsilon = -1.055 \times 10^{-2} + 1.657 \times 10^{-4}T - 1.864 \times 10^{-8}T^2 \tag{3}$$

where T is in K.
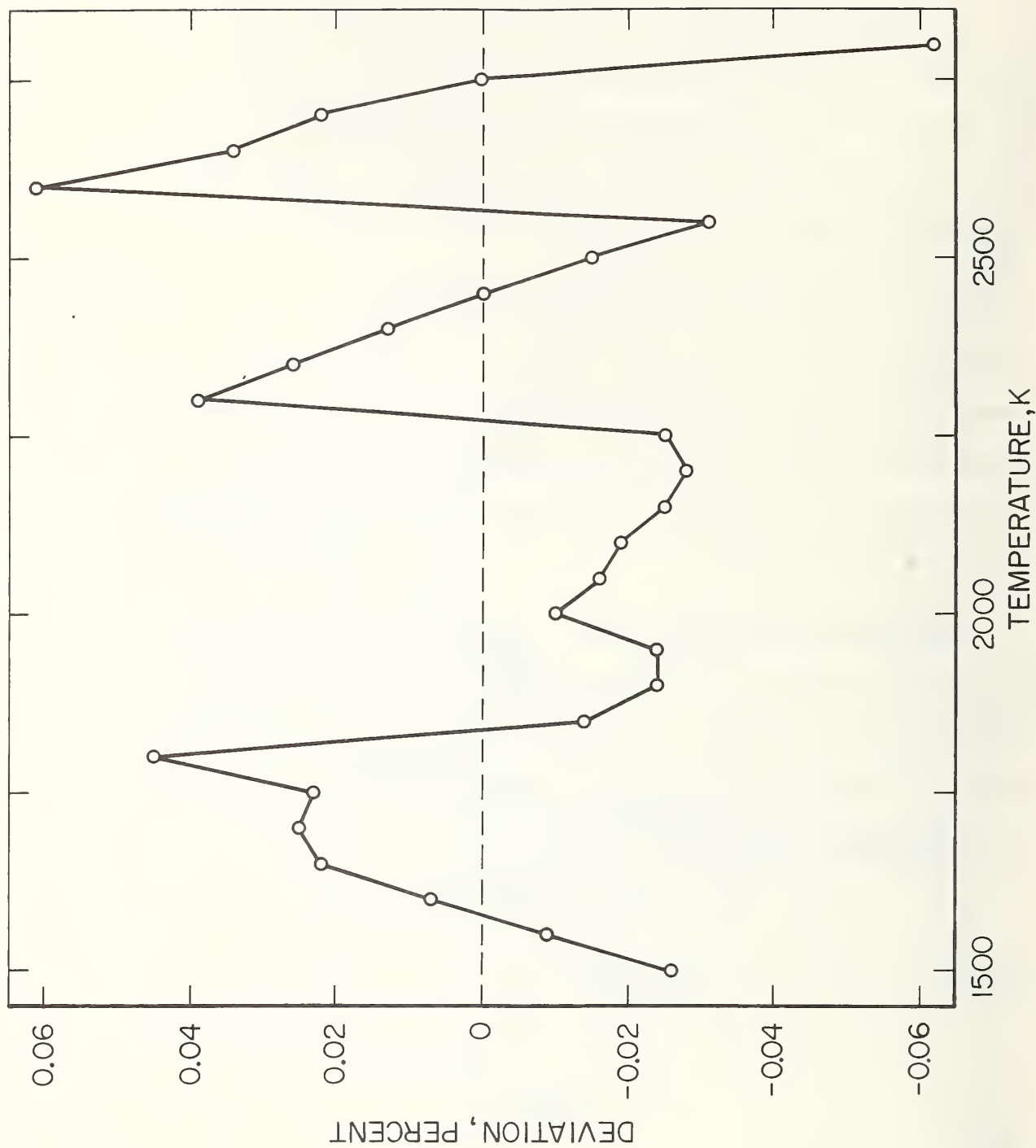
FIGURE 2.   Deviation of electrical resistivity results from equation (2).

Estimate of Errors: The details for estimating errors in
measured and computed quantities in transient experiments using
the present measurement system are given in an earlier publication
[2]. In this paper, the specific items in the error analysis were
recomputed whenever the present conditions differed from those in
the earlier publication. The results for imprecision[3] and
inaccuracy[4] in the properties are: 0.4% and 3% for specific heat,
0.03% and 0.5% for electrical resistivity, 0.6% and 3% for
hemispherical total emittance.

4. Discussion

The specific heat, electrical resistivity and hemispherical
total emittance of the ternary alloy niobium (80) - tantalum (10) -
tungsten (10) alloy measured in this work are presented graphically
in figures 3, 4, and 5, respectively. For comparison purposes,
similar results for niobium, tantalum and tungsten metals, measured
and reported earlier [4, 5, 6] are also included in the figures.

---

[3] Imprecision refers to the standard deviation of an individual point
as computed from the difference between measured value and that from
the smooth function obtained by the least squares method.

[4] Inaccuracy refers to the estimated total error (random and systematic).
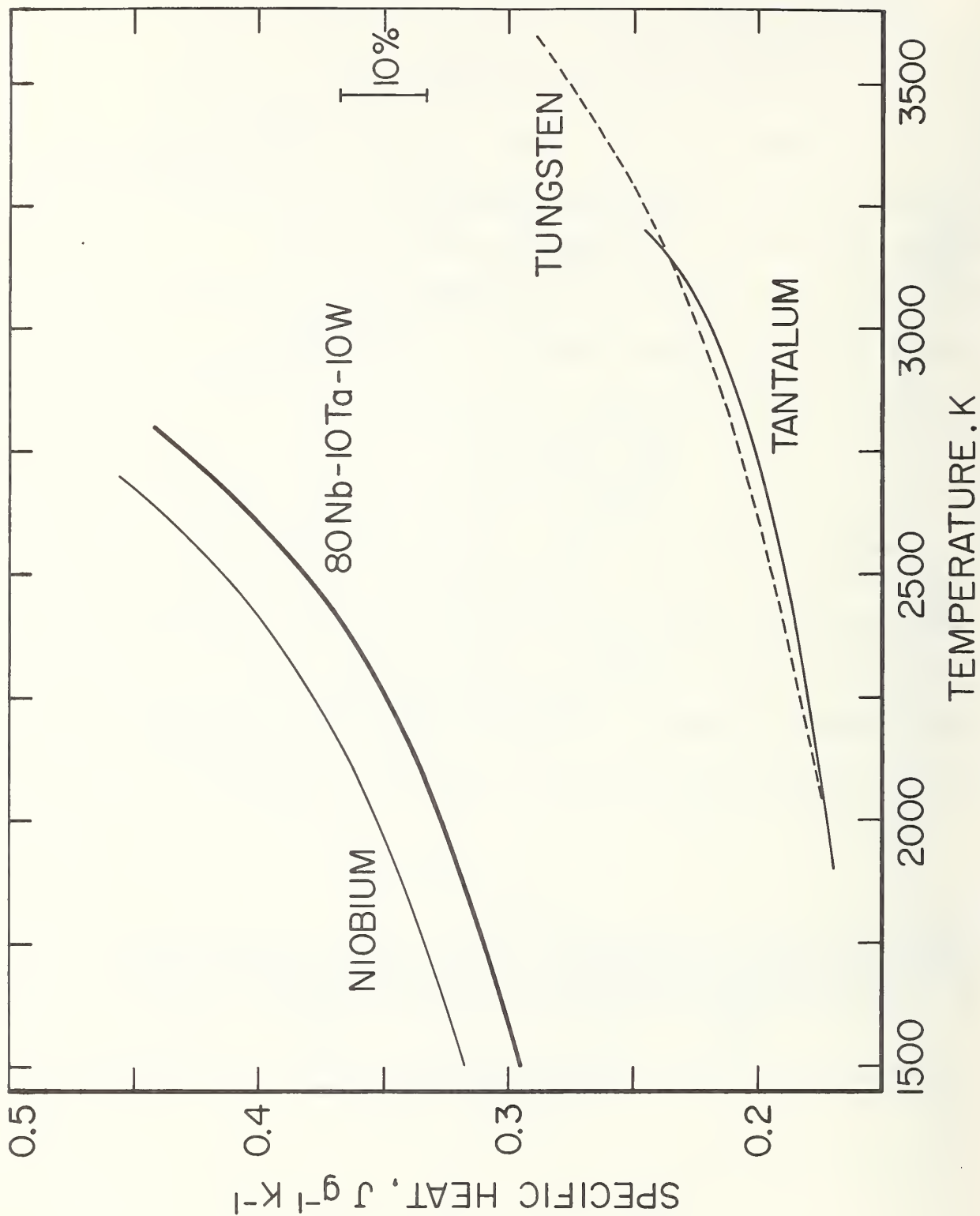
FIGURE 3. Specific heat of the ternary alloy 80Nb-10Ta-10W and the constituent elements.
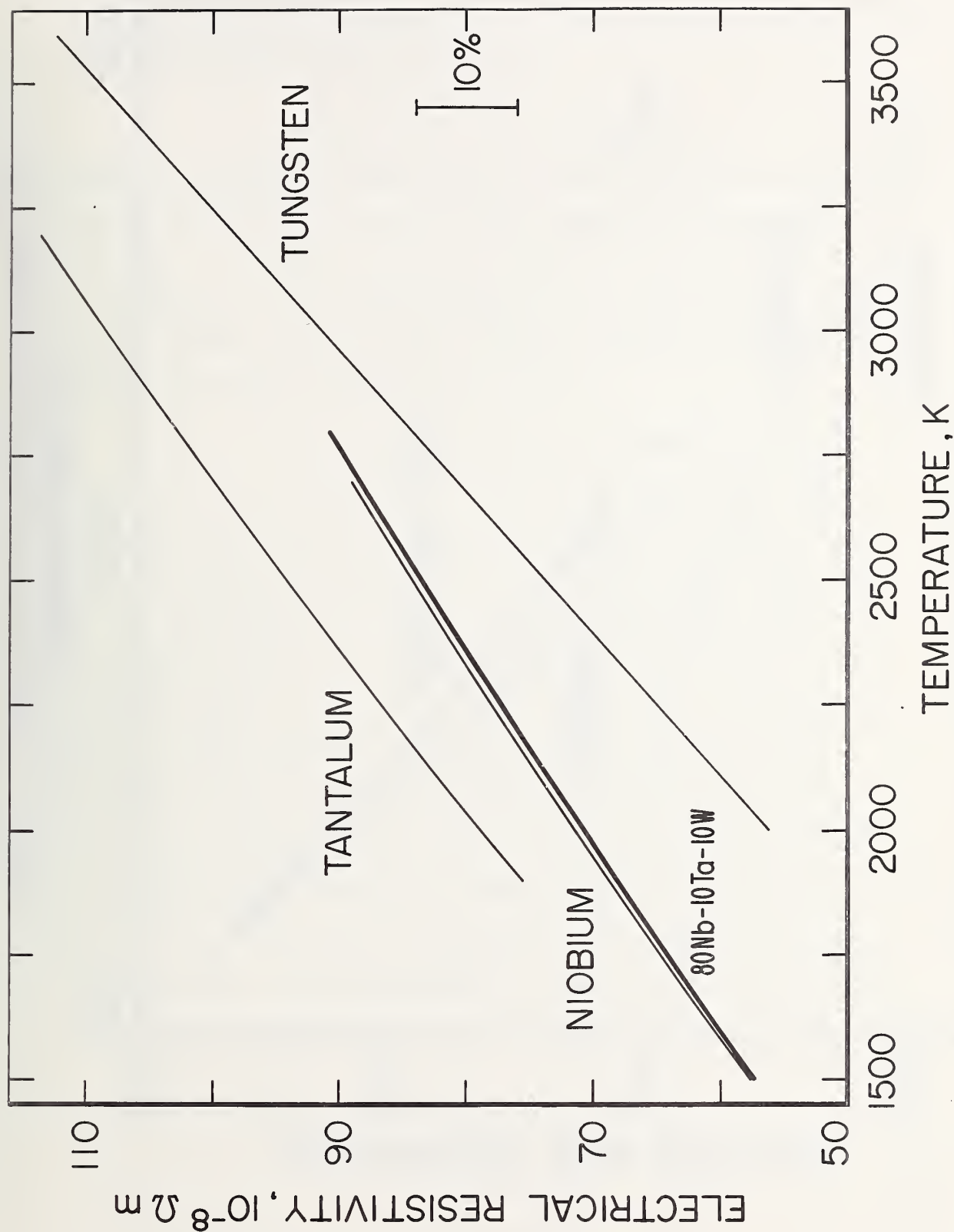
FIGURE 4.   Electrical resistivity of the ternary alloy 80Nb-10Ta-10W and the constituent elements.

11
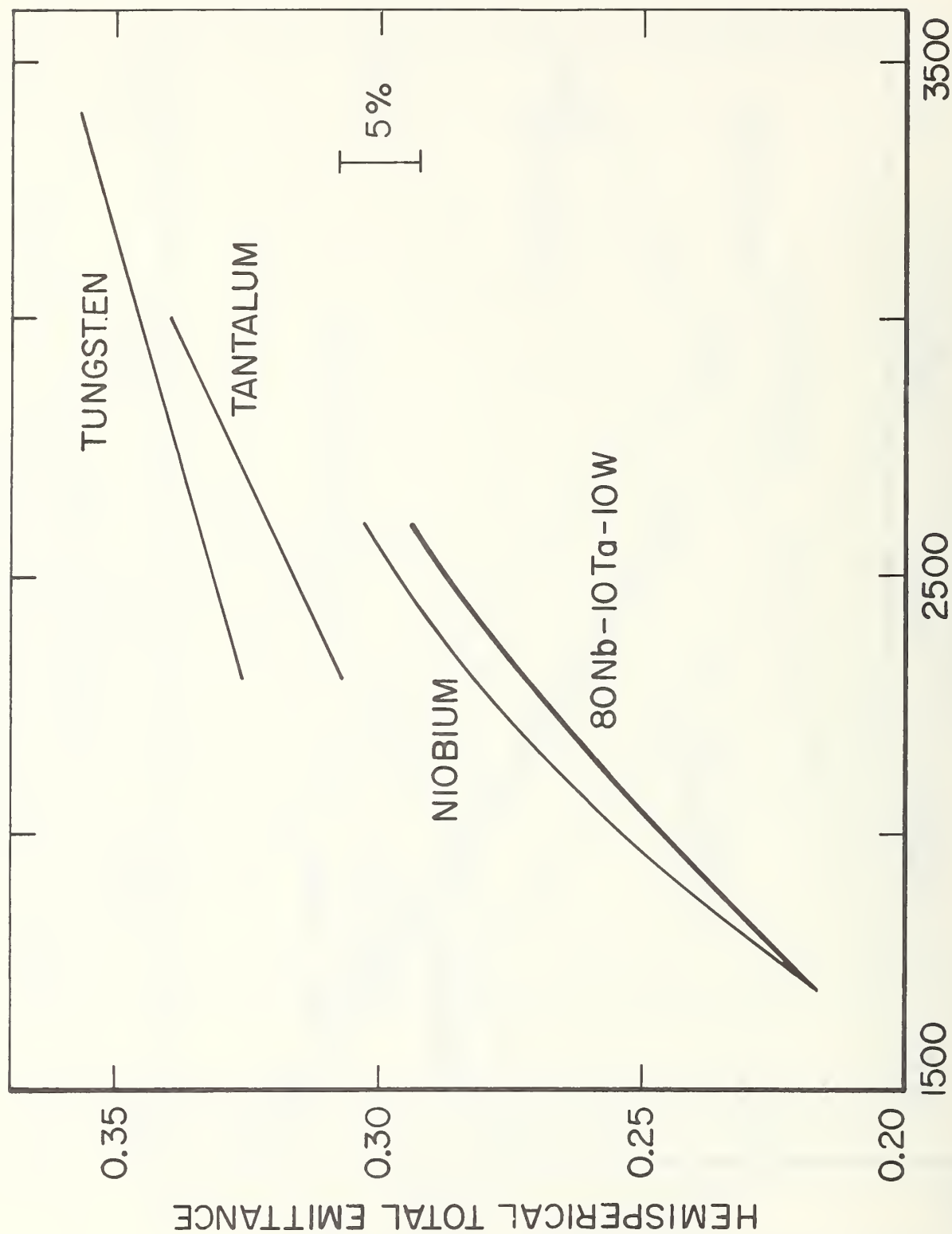
FIGURE 5.   Hemispherical total emittance of the ternary alloy
80Nb-10Ta-10W and the constituent elements.

12

According to Kopp's law, specific heat of a ternary alloy, c_{123} (on mass basis), may be expressed as

$$c_{123} = x_1 c_1 + x_2 c_2 + x_3 c_3 \tag{4}$$

where x_1, x_2 and x_3 are mass fractions of the constituent elements 1, 2 and 3, and c_1, c_2 and c_3 are their respective specific heats.

Departure of the measured specific heat of this work from Kopp's law was computed using the data on niobium, tantalum and tungsten reported in earlier publications [4, 5, 6].

The results are presented graphically in figure 6. It may be seen that in the temperature interval 2000 to 2800 K (interval in which data on the three constituent elements are available) the measured values are approximately 2.6% (on the average) higher than the computed values. The results of earlier measurements [7] of the specific heat of the binary alloy tantalum (90) - tungsten (10) have also shown a similar trend, that is, the measured values of the alloy were approximately 2% higher than the computed values according to the Kopp's law. However, too much significance should not be placed to the difference between measured and computed specific heat values since its magnitude is less than the combined estimated errors in the measurements of specific heat of the alloy and its   constituents.

13
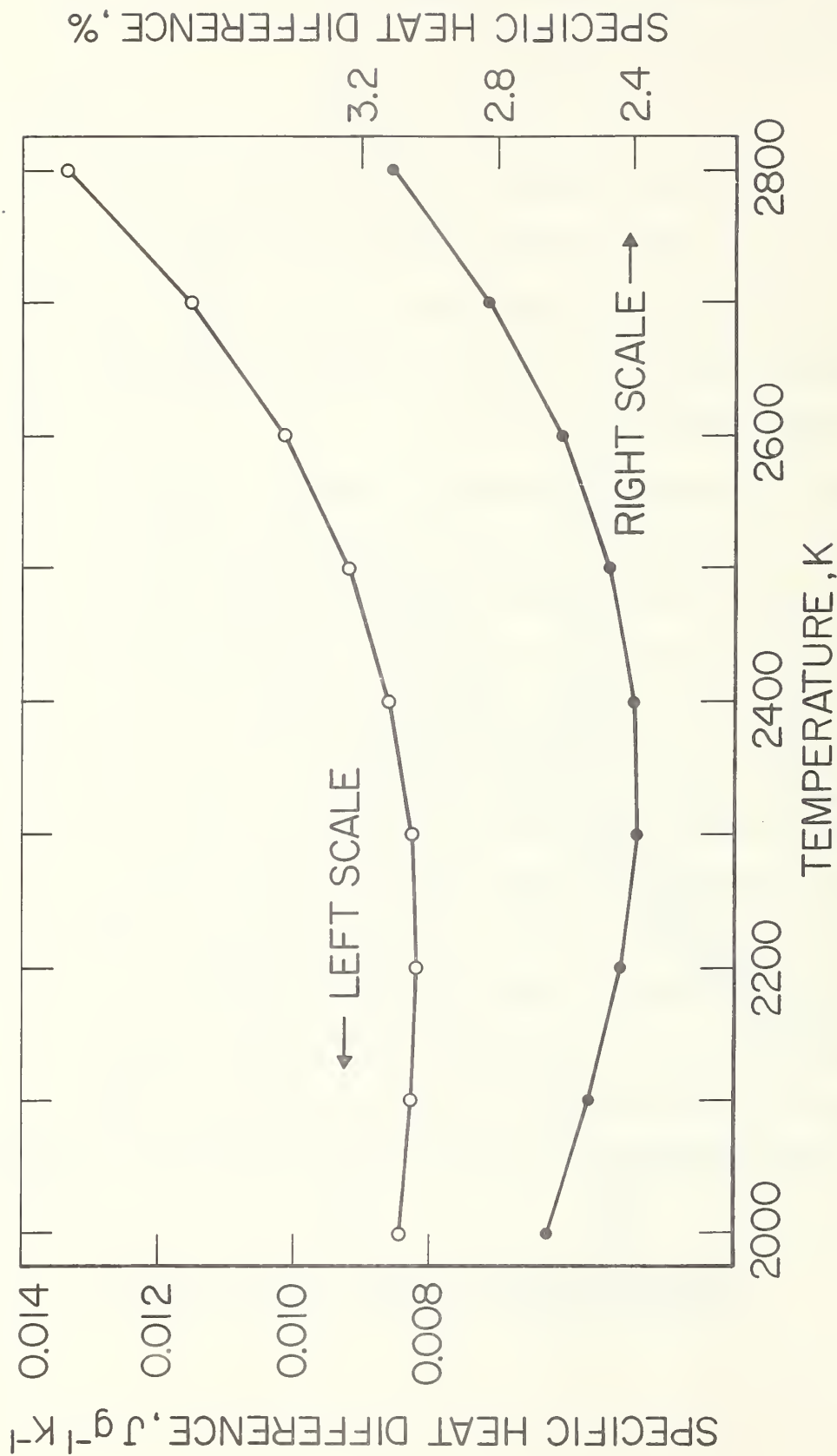
FIGURE 6. Departure of the specific heat of the ternary alloy 80Nb-10Ta-10W from Kopp's law. Specific heat difference refers to measured values minus computed values according to Equation (4).

The Matthiessen's law for the electrical resistivity of a ternary alloy, ρ_{123}, may be expressed as

$$\rho_{123} = X_1\rho_1 + X_2\rho_2 + X_3\rho_3 + \rho_o \tag{5}$$

where X_1, X_2 and X_3 are atomic fractions of the constituent elements 1, 2 and 3, and ρ_1, ρ_2 and ρ_3 are their respective electrical resistivities. The quantity ρ_o is considered to be constant (temperature independent) for a given alloy.

Rearrangement of Equation (5) yields

$$\rho_o = \rho_{123} - (X_1\rho_1 + X_2\rho_2 + X_3\rho_3) \tag{6}$$

Departure of the electrical resistivity of the ternary alloy of this work from Matthiessen's law is determined using Equation (6). The measured values for the alloy are substituted for ρ_{123} and data on niobium, tantalum and tungsten reported in earlier publications [4, 5, 6] are used for ρ_1, ρ_2 and ρ_3. The results are presented graphically in figure 7 in terms of the quantity ρ_o. According to the law, ρ_o should be constant, however computations show that it decreases with increasing temperature and undergoes sign reversal at high temperatures. The two curves in figure 7 were obtained by fitting the high temperature points to linear and quadratic functions using the least squares method, and forcing the functions to pass through the room temperature value. Average absolute difference of the points from the linear and quadratic functions is 0.02×10^{-8} Ω m and 0.1×10^{-8} Ω m, respectively. Since either one of these values

15
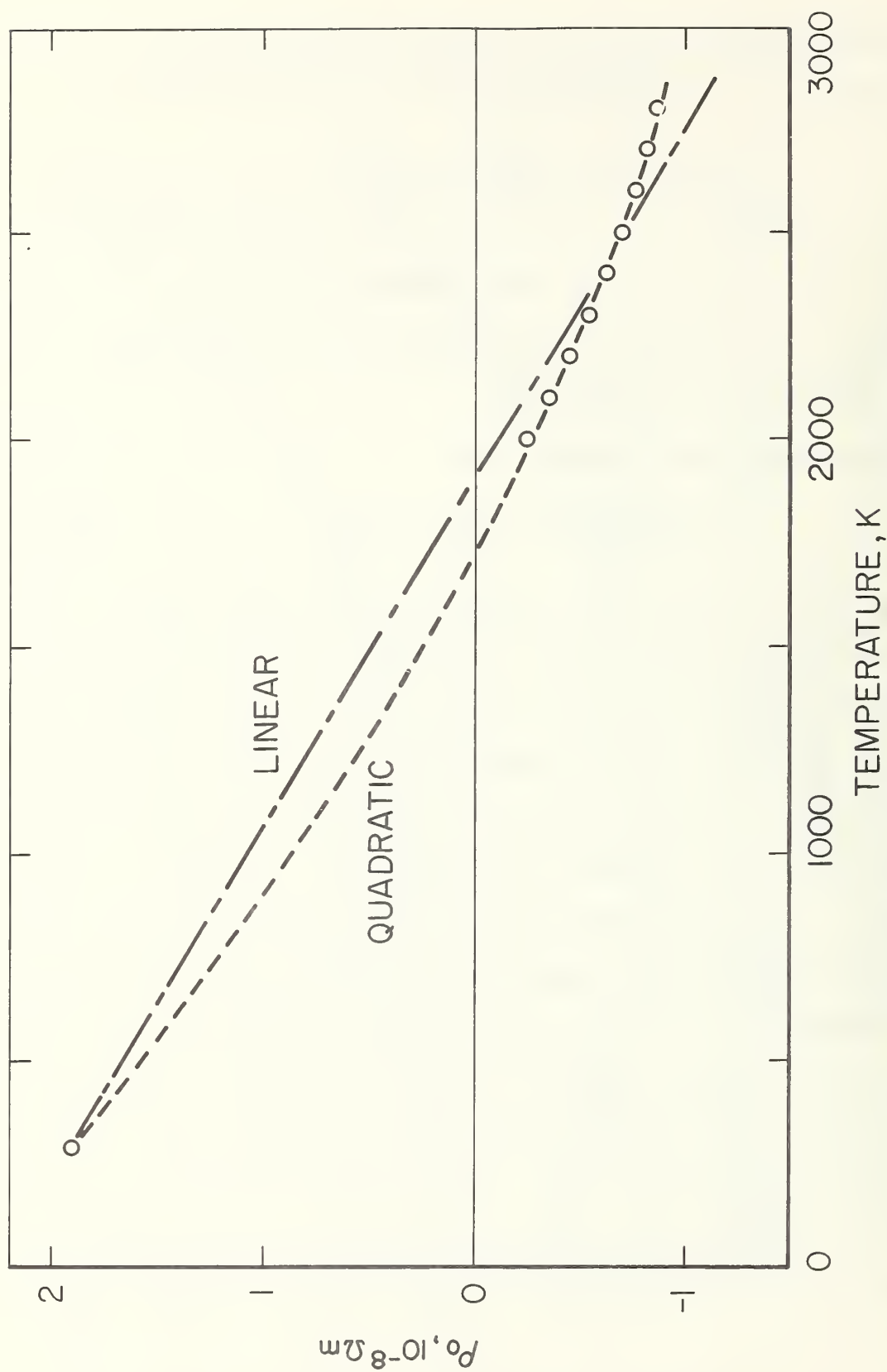
FIGURE 7. Variation of the quantity ρ_o, defined by equation (6), as a function of temperature for the ternary alloy 80Nb-10Ta-10W.

16

is considerably less than the estimated uncertainty of the individual points ($1.1 \times 10^{-8} \Omega$ m, which is obtained from the combination of estimated errors in the electrical resistivity of the alloy and its three constituents) the form of the function (linear or quadratic) is not significant. However, the general trend, that is decrease in the quantity ρ_o with increasing temperature, is significant.

At 293 K, electrical resistivity of the alloy ($17.2 \times 10^{-8} \Omega$ m is higher than the resistivity of any one of its constituents ($15.9 \times 10^{-8} \Omega$ m for niobium, $14.0 \times 10^{-8} \Omega$ m for tantalum and $5.45 \times 10^{-8} \Omega$ m for tungsten). However, at high temperatures (figure 4) the resistivity of the alloy is lower than that of the major constituent, niobium. A similar trend was also observed in the electrical resistivity of the binary alloy tantalum (90) - tungsten (10) reported earlier [7]. Like niobium, at high temperatures the alloy showed a negative departure from linearity in the curve of electrical resistivity versus temperature.

Acknowledgement

5. Appendix

Table A-1

Experimental results on specific heat and

electrical resistivity of the ternary alloy

niobium (80) - tantalum (10) - tungsten (10)

T (K)	c_p (J g^{-1}K^{-1})	Δc_p[a] (%)	ρ ($10^{-8}\Omega$ m)	$\Delta \rho$[a] (%)
1500	0.2947	+0.18	57.25	-0.03
1550	0.2972	-0.17	58.64	-0.01
1600	0.3011	+0.04	60.02	+0.01
1650	0.3064	+0.73	61.39	+0.02
1700	0.3058	-0.50	62.75	+0.03
1750	0.3098	-0.18	64.10	+0.02
1800	0.3138	+0.11	65.46	+0.05
1850	0.3134	-1.01	66.76	-0.01
1900	0.3187	-0.35	68.09	-0.02
1950	0.3240	+0.26	69.41	-0.02
2000	0.3289	+0.69	70.74	0
2050	0.3299	-0.14	72.04	-0.02
2100	0.3342	-0.05	73.34	-0.02
2150	0.3391	+0.12	74.64	-0.03
2200	0.3446	+0.37	75.93	-0.03
2250	0.3509	+0.72	77.21	-0.03
2300	0.3535	-0.10	78.54	+0.04
2350	0.3594	-0.10	79.80	+0.03
2400	0.3658	-0.13	81.06	+0.01
2450	0.3725	-0.20	82.30	0
2500	0.3798	-0.29	83.54	-0.02
2550	0.3877	-0.39	84.77	-0.03
2600	0.3983	+0.03	86.09	+0.06
2650	0.4082	+0.08	87.30	+0.03
2700	0.4187	+0.08	88.51	+0.02
2750	0.4300	+0.07	89.71	0
2800	0.4422	+0.07	90.87	-0.06

[a]The quantities Δc_p and $\Delta \rho$ are percentage deviations of the individual results from the smooth functions represented by equations (1) and (2), respectively.

Table A-2

Experimental results on hemispherical total emittance

of the ternary alloy niobium (80) - tantalum (10) - tungsten (10)

T (K)	ϵ	$\Delta\epsilon$[a] (%)
1693.2	0.2171	+0.23
1693.6	0.2158	-0.39
1693.7	0.2186	+0.89
1694.1	0.2180	+0.60
1885.0	0.2329	-1.15
1885.6	0.2326	-1.31
1885.6	0.2356	-0.02
1886.2	0.2360	+0.13
2053.0	0.2512	+0.04
2053.9	0.2506	-0.23
2053.9	0.2519	+0.29
2054.8	0.2516	+0.14
2333.2	0.2748	+0.07
2334.7	0.2753	+0.21
2334.7	0.2757	+0.35
2336.2	0.2764	+0.56
2663.2	0.2976	-0.32
2665.6	0.2981	-0.21
2665.6	0.2986	-0.04
2668.0	0.2993	+0.14

[a]The quantity $\Delta\epsilon$ is percentage deviation of the individual results from the smooth function represented by equation (3).

6. References

[1]   Cezairliyan, A., Design and operational characteristics of
       a high-speed (millisecond) system for the measurement of
       thermophysical properties at high temperatures, J. Res. Nat.
       Bur. Stand. (U. S.), 75C (Eng. and Instr.), 7 (1971).

[2]   Cezairliyan, A., Morse, M. S., Berman, H. A., and Beckett, C. W.,
       High-speed (subsecond) measurement of heat capacity, electrical
       resistivity, and thermal radiation properties of molybdenum
       in the range 1900 to 2800 K, J. Res. Nat. Bur. Stand.
       (U. S.), 74A (Phys. and Chem.), 65 (1970).

[3]   International Practical Temperature Scale of 1968, Metrologia,
       5, 35 (1969).

[4]   Cezairliyan, A., High-speed (subsecond) measurement of heat
       capacity, electrical resistivity, and thermal radiation
       properties of niobium in the range 1500 to 2700 K, J. Res.
       Nat. Bur. Stand. (U. S.), 75A (Phys. and Chem.), 565 (1971).

[5]   Cezairliyan, A., McClure, J. L., and Beckett, C. W., High-
       speed (subsecond) measurement of heat capacity, electrical
       resistivity, and thermal radiation properties of tantalum
       in the range 1900 to 3200 K, J. Res. Nat. Bur. Stand. (U. S.),
       75A (Phys. and Chem.), 1 (1971).

[6]   Cezairliyan, A., and McClure, J. L., High-speed (subsecond) measurement of heat capacity, electrical resistivity, and thermal radiation properties of tungsten in the range 2000 to 3600 K, J. Res. Nat. Bur. Stand. (U. S.), 75A (Phys. and Chem.), 283 (1971).

[7]   Cezairliyan, A., High-speed (subsecond) simultaneous measurement of specific heat, electrical resistivity, and hemispherical total emittance of tantalum-10 (wt. %) tungsten alloy in the range 1500 to 3200 K, High Temperatures-High Pressures, 4, 541 (1972).

Chapter 2

THERMOPHYSICAL MEASUREMENTS ON IRON AEOVE 1500 K

USING A TRANSIENT (SUBSECOND) TECHNIQUE

A. Cezairliyan and J. L. McClure
Institute for Materials Research
National Bureau of Standards
Washington, DC 20234

Abstract

Simultaneous measurements of heat capacity, electrical resistivity and hemispherical total emittance of iron (99.9$^+$% pure) in the temperature range 1500 to 1800 K, and the melting point of iron by a subsecond duration, transient technique are described. The measurements indicate increases in heat capacity and electrical resistivity as the result of the solid-solid phase transformation ($\gamma \rightarrow \delta$) in iron. The measured value of the hemispherical total emittance at 1720 K is 0.33. The average of the results of two experiments yield a value of 1808 K for the melting point of iron. Estimated inaccuracies of measured properties are: 3% for heat capacity and emittance, 1% for electrical resistivity, and 5 K for the melting point.

1. Introduction

Most of the reliable measurements of thermophysical and related properties of iron reported in the literature were performed at temperatures below 1500 K. Even at these temperatures, considerable disagreements exist between the results of various investigations. To a large extent, these disagreements may be attributed to difficulties associated with the magnetic and allotropic transformations in iron. The objective of the present work is to measure selected properties (heat capacity, electrical resistivity, hemispherical total emittance and melting point) of iron above 1500 K using a transient technique.

The method is based on rapid resistive self-heating of the specimen from room temperature to high temperatures in less than one second by the passage of an electrical current pulse through it; and on measuring with millisecond resolution, such experimental quantities as current through the specimen, potential drop across the specimen, and specimen temperature. Details regarding the construction and operation of the measurement system, the formulation of relations for the properties, the methods of measuring experimental quantities, and other pertinent information are given in earlier publications [1,2][1].

2. Measurements

Specimens: The specimens were tubes fabricated from rods[2] by removing the center portion using an electro-erosion technique. The

---

[1]Figures in brackets indicate the literature references at the end of this paper.

[2]The specimens in rod form were furnished by the Office of Standard Reference Materials (OSRM) of NBS (Standard Reference Material 734-S, Electrolytic Iron, 99.9$^+$% pure). The details regarding the impurities are documented by OSRM.

nominal dimensions of the specimens were: length, 102 mm; outside
diameter, 6.3 mm; and wall thickness, 0.5 mm. The outer surface of the
specimens were polished to reduce heat loss due to thermal radiation.

Procedure: Because of the existence of a solid-solid phase trans-
formation ($\gamma \rightarrow \delta$) in iron at approximately 1682 K, the measurements were
performed in the following two ranges: low (1500–1660 K), and high
(1700–1800 K). Four experiments were conducted on two specimens; two
experiments in the low range and two experiments in the high range.
The duration of the current pulses in the experiments ranged from 500
to 900 ms, and the heating rate ranged from 2000 to 3500 K s^{-1}.
Radiative heat loss from the specimen was, in all cases, less than 2%
at 1500 K and less than 4% at 1800 K of the input power. All the
experiments were conducted with the specimen in a vacuum environment
of approximately 10^{-5} torr.

3. Experimental Results

The properties reported in this paper are based on the International
Practical Temperature Scale of 1968 [3]. In all computations, the geo-
metrical quantities are based on their room temperature (298 K) dimen-
sions. The experimental results for the heat capacity and the electrical
resistivity of iron (for each phase) are presented as linear functions
in temperature. These functions were obtained by least squares approxi-
mation of the individual points corresponding to the measurements on the
two specimens. The final values of the properties at 20 degree tempera-
ture intervals computed from these functions are presented in table 1.
The results of individual experiments are given in the Appendix.

TABLE 1

Heat capacity and electrical resistivity of iron

	Temp. K	c_p J mol^{-1} K^{-1}	ρ 10^{-8} Ω m
γ-iron	1500	36.12	120.66
	1520	36.37	121.10
	1540	36.61	121.54
	1560	36.86	121.98
	1580	37.11	122.42
	1600	37.35	122.86
	1620	37.60	123.29
	1640	37.84	123.73
	1660	38.09	124.17
δ-iron	1700	41.46	125.35
	1720	42.09	125.65
	1740	42.72	125.96
	1760	43.35	126.26
	1780	43.99	126.57
	1800	44.62	126.87

Heat Capacity: Heat capacity was computed from data taken during
the heating period. A correction for power loss due to thermal radiation
was made using the single measured value of hemispherical total emittance
in conjunction with the slope of emittance versus temperature function
obtained from the literature [4].

The functions for heat capacity are:

In the temperature range 1500 to 1660 K (γ-iron),

$$c_p = 17.64 + 1.232 \times 10^{-2} \, T \tag{1}$$

In the temperature range 1700 to 1800 K (δ-iron),

$$c_p = -12.28 + 3.161 \times 10^{-2} \, T \tag{2}$$

where T is in K, and c_p is in J mol^{-1} K^{-1}. The standard deviation for
equations (1) and (2) is 0.4%. In the computations of heat capacity,
the atomic weight of iron was taken as 55.85.

Electrical Resistivity: The electrical resistivity was determined
from the same experiments that were used to calculate the heat capacity.

The functions for electrical resistivity are:

In the temperature range 1550 to 1660 K (γ-iron),

$$\rho = 87.72 + 2.196 \times 10^{-2} \, T \tag{3}$$

In the temperature range 1700 to 1800 K (δ-iron),

$$\rho = 99.37 + 1.528 \times 10^{-2} \, T \tag{4}$$

where T is in K and ρ is in 10^{-8} Ω m. The standard deviation for equations
(3) and (4) is 0.5%. The electrical resistivity of one of the specimens
measured at 293 K using a Kelvin bridge was 10.2×10^{-8} Ω m.

Hemispherical Total Emittance: In one of the experiments in the
lower temperature range data were taken during the initial cooling period

26

TIME, ARBITRARY UNIT

TEMPERATURE, K

1810

1800

1790

1780

0

10

20

30

3K

1808.6 K – – –
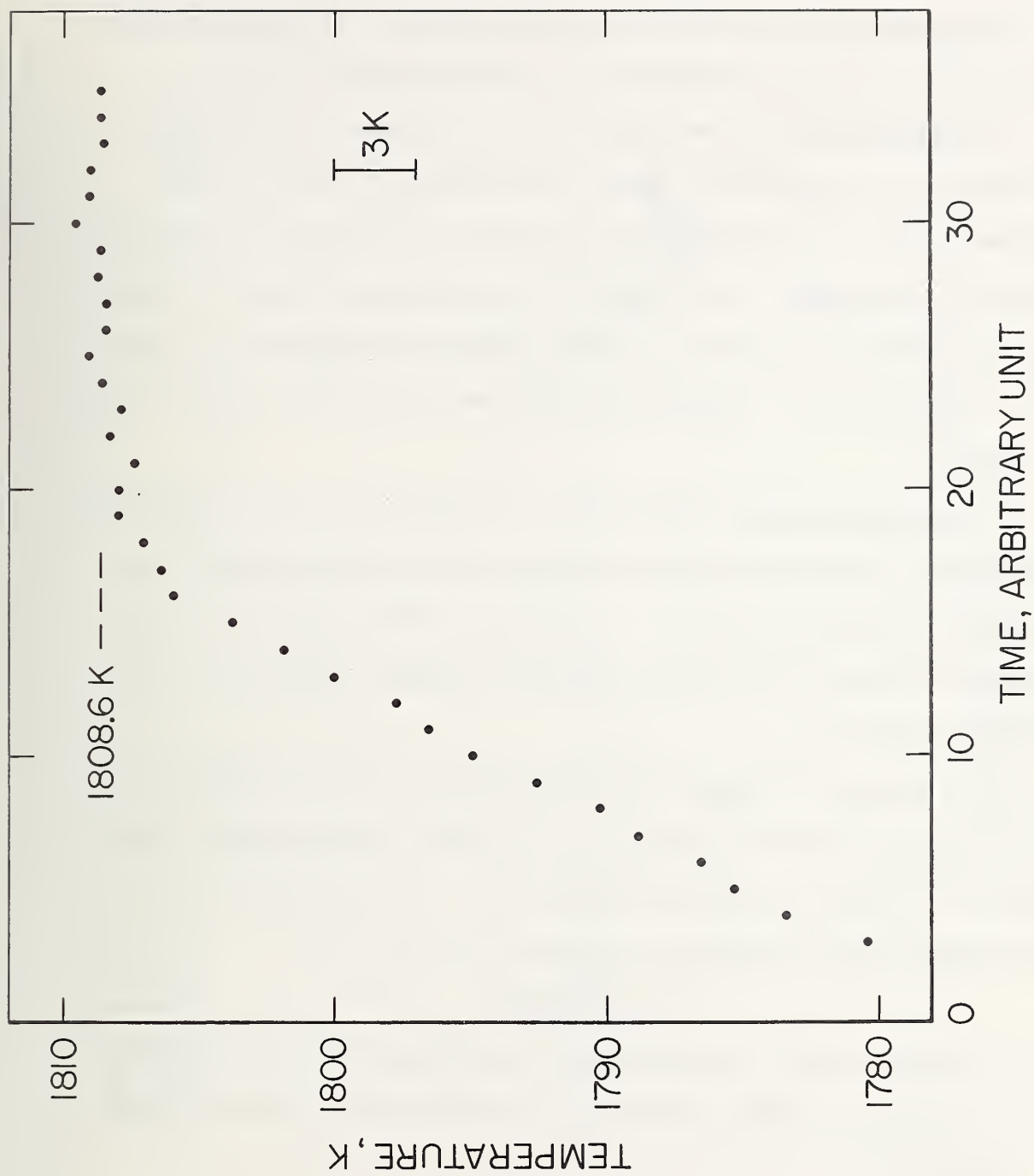
FIGURE 1. Variation of temperature of iron (specimen-2) as a function of time near and at the melting point (1 time unit = 0.833 ms).

27

of the specimen which followed the heating period. The results yielded a value of 0.33 for the hemispherical total emittance at 1720 K.

Melting Point: The melting point of a specimen is manifested by a plateau in the temperature versus time function (figure 1). The melting point of the specimen was determined by averaging the temperature points at the plateau. The results for two specimens (figure 2) yielded the values 1807.5 K and 1808.6 K, with standard deviations of 0.2 K and 0.4 K, respectively. It may be concluded that the melting point of iron is 1808 K.

Estimate of Errors: The details for estimating errors in measured and computed quantities using the present measurement system are given in an earlier publication [2]. In this paper, the specific items were recomputed whenever the present conditions differed from those in the earlier publication.

The results for imprecision[3] and inaccuracy[4] in the properties are: 0.6% and 3% for heat capacity, 0.5% and 1% for electrical resistivity, 0.5 K and 5 K for the melting point. The inaccuracy in the hemispherical total emittance is estimated to be 3%.

4. Discussion

The heat capacity and electrical resistivity results of this work are compared graphically with those in the literature in figures 3 and 4, respectively.

---

[3]Imprecision refers to the standard deviation of an individual point as computed from the difference between measured value and that from the smooth function obtained by the least squares method.

[4]Inaccuracy refers to the estimated total error (random and systematic).
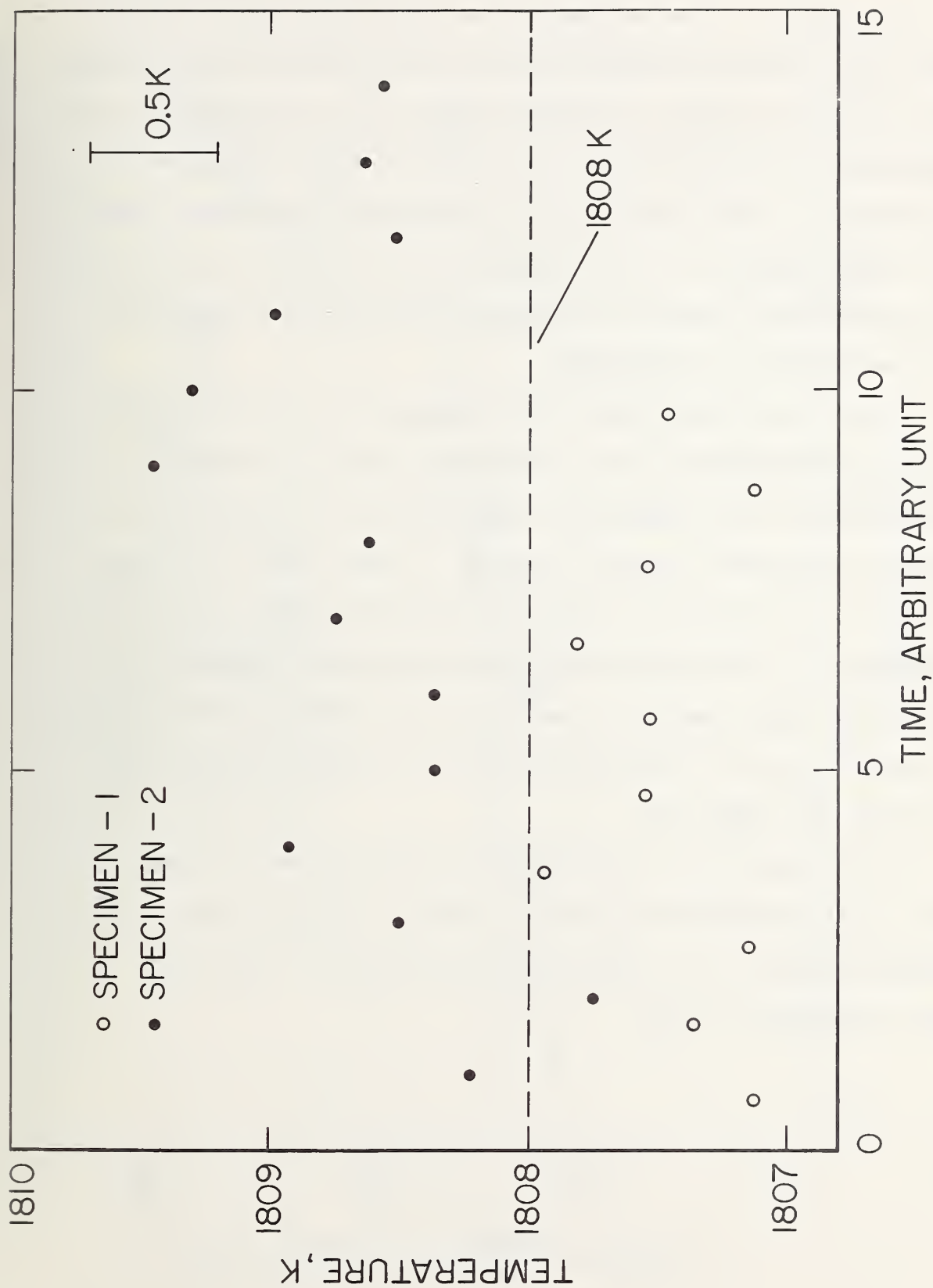
FIGURE 2. Variation of temperatures of two iron specimens as a function of time at the melting point (1 time unit = 0.833 ms).

From figure 3 it may be seen that at 1300 K considerable disagreements (up to approximately 10%) exist in the heat capacity values reported in the literature; however, immediately below the $\gamma \rightarrow \delta$ transformation the disagreements (especially between the results of recent investigations) are reduced to a value less than 3%. In contrast to the constant values for the heat capacity of δ-iron reported in the literature, the results of the present work show that heat capacity increases with temperature as the melting point is approached.

Figures 3 and 4 show that the heat capacity and electrical resistivity are discontinuous at the transformation point. Extrapolation of the properties to the transformation temperature (1682 K, based on preliminary measurements) indicates increases of approximately 7% in the heat capacity and 0.3% in the electrical resistivity during the $\gamma \rightarrow \delta$ transformation. The actual increase in the electrical resistivity is likely to be larger than this value because the expansion that occurs in iron during the $\gamma \rightarrow \delta$ transformation was not included in the electrical resistivity computations.

The melting point of iron reported in the literature is given in table 2. All the tabulated values are within 6 K of each other. The maximum difference of the present value from the values reported by other investigators is 4 K.
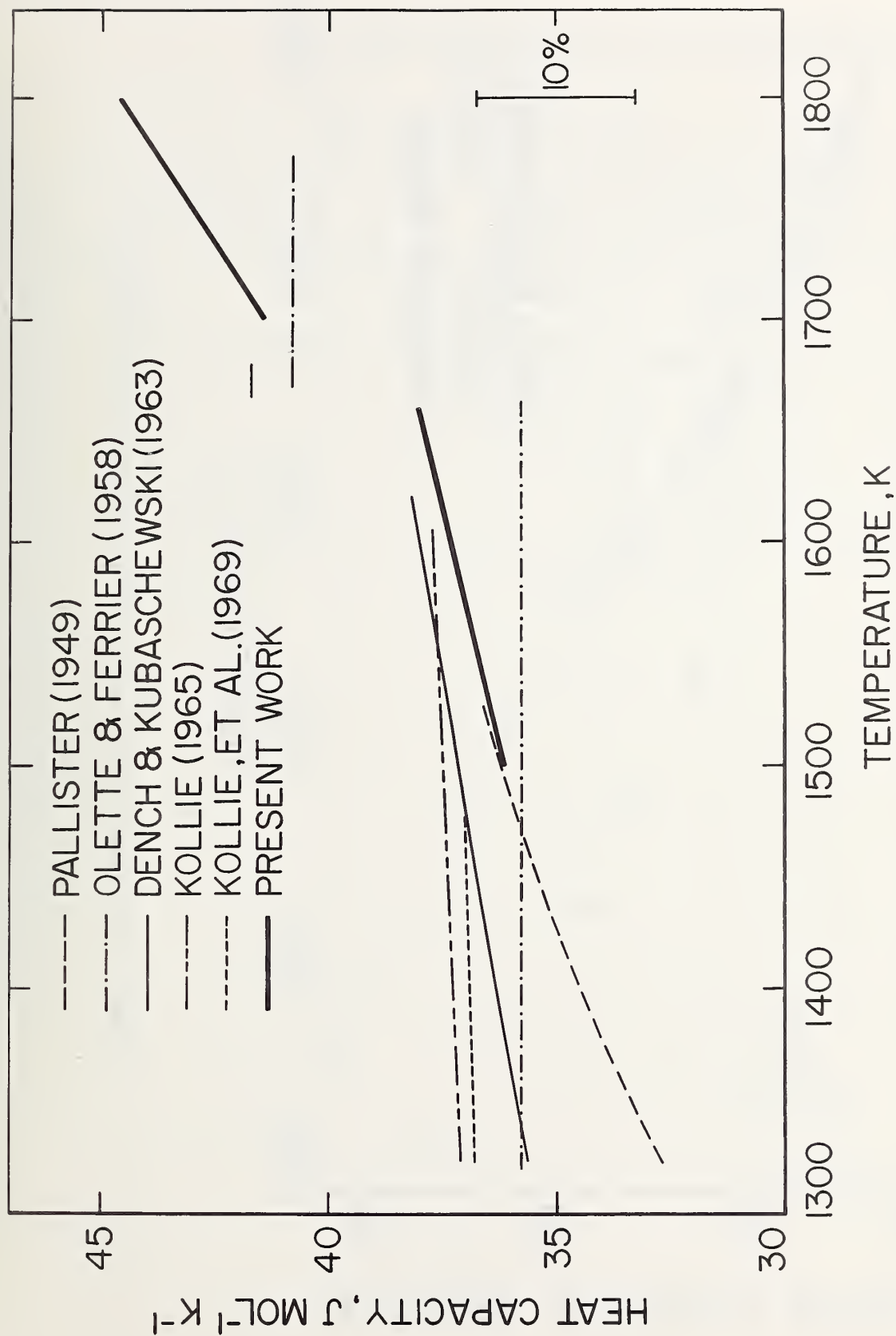
FIGURE 3. Heat capacity of iron reported in the literature.

31
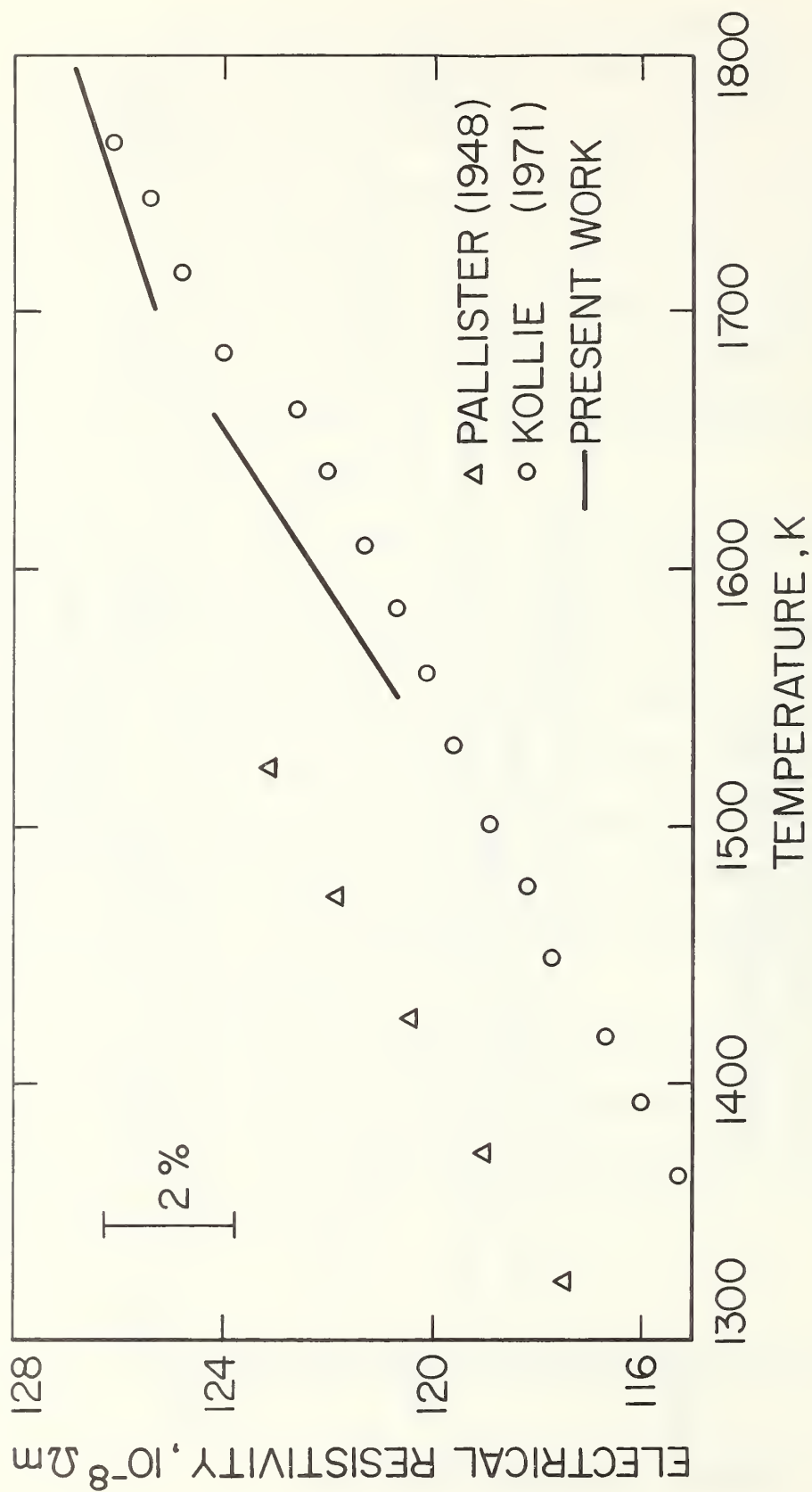
FIGURE 4. Electrical resistivity of iron reported in the literature.

TABLE 2

Melting point of pure iron

Investigator	Ref.	Year	Melting Point,[*] K
Bristow	11	1939	1806 ± 5
Chipman & Marshall	12	1940	1807
Roeser & Wensel	13	1942	1812 ± 1
Schofield & Bacon	14	1953	1810 ± 10
Present Work			1808 ± 5

[*]All temperatures are corrected to the IPTS 1968.

Appendix

Table A-1

Experimental results on heat capacity and electrical resistivity of iron[*]

	Temp. K	Specimen-1		Specimen-2	
		c_p	ρ	c_p	ρ
γ-iron	1500	35.87	121.12	36.38	120.13
	1520	36.12	121.59	36.62	120.59
	1540	36.37	122.05	36.85	121.04
	1560	36.62	122.51	37.08	121.49
	1580	36.88	122.95	37.31	121.92
	1600	37.14	123.39	37.54	122.35
	1620	37.40	123.82	37.78	122.76
	1640	37.67	124.25	38.01	123.17
	1660	37.94	124.66	38.27	123.56
δ-iron	1700	41.37	125.80	41.66	124.87
	1720	41.95	126.13	42.22	125.22
	1740	42.58	126.45	42.83	125.54
	1760	43.18	126.71	43.48	125.83
	1780	43.81	127.07	44.13	126.08
	1800	44.51	127.38	44.86	126.30

[*]Heat capacity in J mol^{-1} K^{-1}, electrical resistivity in 10^{-8} Ωm.

34

5. References

[1] Cezairliyan, A., Design and operational characteristics of a high-speed (millisecond) system for the measurement of thermophysical properties at high temperatures, J. Res. Nat. Bur. Stand. (U.S.), 75C (Eng. and Instr.), 7 (1971).

[2] Cezairliyan, A., Morse, M. S., Berman, H. A., and Beckett, C. W., High-speed (subsecond) measurement of heat capacity, electrical resistivity, and thermal radiation properties of molybdenum in the range 1900 to 2800 K, J. Res. Nat. Bur. Stand. (U.S.), 74A (Phys. and Chem.), 65 (1970).

[3] International Practical Temperature Scale of 1968, Metrologia, 5, 35 (1969).

[4] Touloukian, Y. S., and DeWitt, D. P., Thermal radiative properties-metallic elements and alloys, Thermophysical Properties of Matter, Vol. 7, Plenum, New York, 1970.

[5] Pallister, P. R., The specific heat and resistivity of high-purity iron up to 1250°C, J. Iron Steel Inst. (London), 161, 87 (1949).

[6] Olette, M., and Ferrier, A., High temperature enthalpy of gamma and delta pure iron, NPL Symposium No. 9, Vol. 2, Paper 4 H. (1958).

[7] Dench, W. A. and Kubaschewski, W., Heat capacity of iron at 800° to 1420°C, J. Iron Steel Inst. (London), 201, 140 (1963).

[8] Kollie, T. G., M. S. Thesis, University of Tennessee (1965).

[9] Kollie, T. G., Barisoni, M., McElroy, D. L., and Brooks, C. R., Pulse calorimetry using a digital voltmeter for transient data acquisition, High Temp.-High Press., 1, 167 (1969).

[10] Kollie, T. G., Private Communication, 1971.

[11] Bristow, C. A., Iron Steel Inst. Spec. Rep., No. 24, 1 (1939).

[12] Chipman, J. and Marshall, S., The equilibrium $FeO + H_2 = Fe + H_2O$ at temperatures up to the melting point of iron, J. Am. Chem. Soc., 62, 299 (1940).

[13] Roeser, Wm. F. and Wensel, H. T., Freezing temperatures of high-purity iron and some steels, J. Res. NBS, 26, 273 (1941).

[14] Schofield, T. H. and Bacon, A. E., The melting point of titanium, J. Inst. Metals, 82, 167 (1953).

Chapter 3

A SUBSECOND PULSE HEATING TECHNIQUE

FOR THE STUDY OF SOLID-SOLID PHASE TRANSFORMATIONS

AT HIGH TEMPERATURES: APPLICATION TO IRON[*]

A. Cezairliyan and J. L. McClure

National Bureau of Standards

Washington, D. C. 20234

Abstract

The feasibility of the application of a rapid pulse heating
technique to studies of solid-solid phase transformations at high
temperatures is demonstrated by measurements on iron at the $\gamma \rightarrow \delta$
transformation point. The measurement system is capable of heating
the specimen from room temperature to its melting point in
less than one second and measuring the pertinent experimental
quantities every 0.4 ms with a full-scale signal resolution of
one part in 8000. Emphasis is placed on the measurement of the
$\gamma \rightarrow \delta$ transformation temperature. Two different types of iron yielded
the values 1673 K and 1683 K for the transformation temperature. As
a by-product of the experimental data, an estimate for the transformation
energy is obtained $(890 \text{ J} \cdot \text{mol}^{-1})$. The measurements of the normal
spectral emittance (at 650 nm) yielded the values: 0.355 at the
melting point, and 0.361 and 0.368 at the transformation point for
the two types of iron.

---

1. Introduction

Accurate measurements of thermophysical properties at high temperatures require special techniques to overcome the difficulties resulting from heat loss, chemical reaction, evaporation, diffusion, etc. that are associated with conventional steady-state and quasi steady-state methods. These problems have largely been solved by the development of a millisecond resolution pulse heating technique [1] which is used to measure selected thermophysical properties of electrical conductors above 1500 K.

The objective of this paper is to demonstrate the applicability of the pulse heating technique to investigations relating to solid-solid phase transformations. Experimental studies were conducted in the region of $\gamma \to \delta$ transformation in iron. The results of measurements of transformation temperature are reported and estimation of transformation energy is discussed. In addition, measurements of normal spectral emittance (at 650 nm) at the transformation and melting points are presented.

2. Method

The method is based on rapid resistive self-heating of the specimen from room temperature to high temperatures (above 1500 K) by the passage of an electrical current pulse through it. During an experiment, which usually lasts less than one second, the current through the specimen, the potential across the specimen, and the specimen temperature are measured as a function of time and are

recorded with a digital data acquisition system. The system is capable of recording data every 0.4 ms with a full-scale signal resolution of approximately one part in 8000. Specimen temperature is measured with a high-speed photoelectric pyrometer [2]. The details regarding the construction and operation of the measurement system are given in earlier publications [1, 3].

3. Measurements

Two types of high purity iron were used; a commercial vacuum melted electrolytic iron (Ferrovac E)[*] and Standard Reference Material 734 electrolytic iron (SRM 734)[**]. A list of the nature and composition of impurities in each type of iron is given in table 1.

Experiments were conducted on five specimens in the form of tubes (T-1 to T-5) and five specimens in the form of rods (R-1 to R-5). The tubes were made from rod stock by removing the center portion using an electroerosion technique. A small rectangular hole was fabricated in the wall of each tube to approximate blackbody conditions. A summary of the type and dimensions of the specimens is given in table 2.

_____

[*] A trade name of Colt Industries Crucible Inc., Syracuse, N. Y. The identification of this material does not imply recommendation or endorsement by the National Bureau of Standards.

[**] The SRM 734 electrolytic iron was furnished in rod form by the Office of Standard Reference Materials (OSRM) of NBS.

Table 1

Impurities in the iron specimens

Impurity	Composition, ppm	
	Ferrovac E	SRM 734
Al	100	7
C	60	67
Co	30	70
Cr	100	72
Cu	10	58
Mn	10	57
Mo	10	50
Ni	300	410
P	30	25
Pb	6	< 1
S	70	59
Si	80	80
Sn	10	< 5
Ti	-	6
V	40	6
W	100	< 1
H_2	1	< 5
N_2	4	< 20
O_2	260	< 70
Total	1221	< 1069

Table 2

Summary of the type and dimensions of the iron specimen

Specimen		Type of Material	Nominal Dimension
Geometry	Designation		
Tube	T-1, T-2	Ferrovac E	Length: 89 mm
	T-3,T-4,T-5	SRM 734	Outside Diameter: 6.4 mm Wall Thickness: 0.5 mm Sighting Hole: 0.5 x 1 mm
Rod	R-1,R-2,R-3	Ferrovac E	Length: 89 mm
	R-4, R-5	SRM 734	Diameter: 3.2 mm

RADIANCE
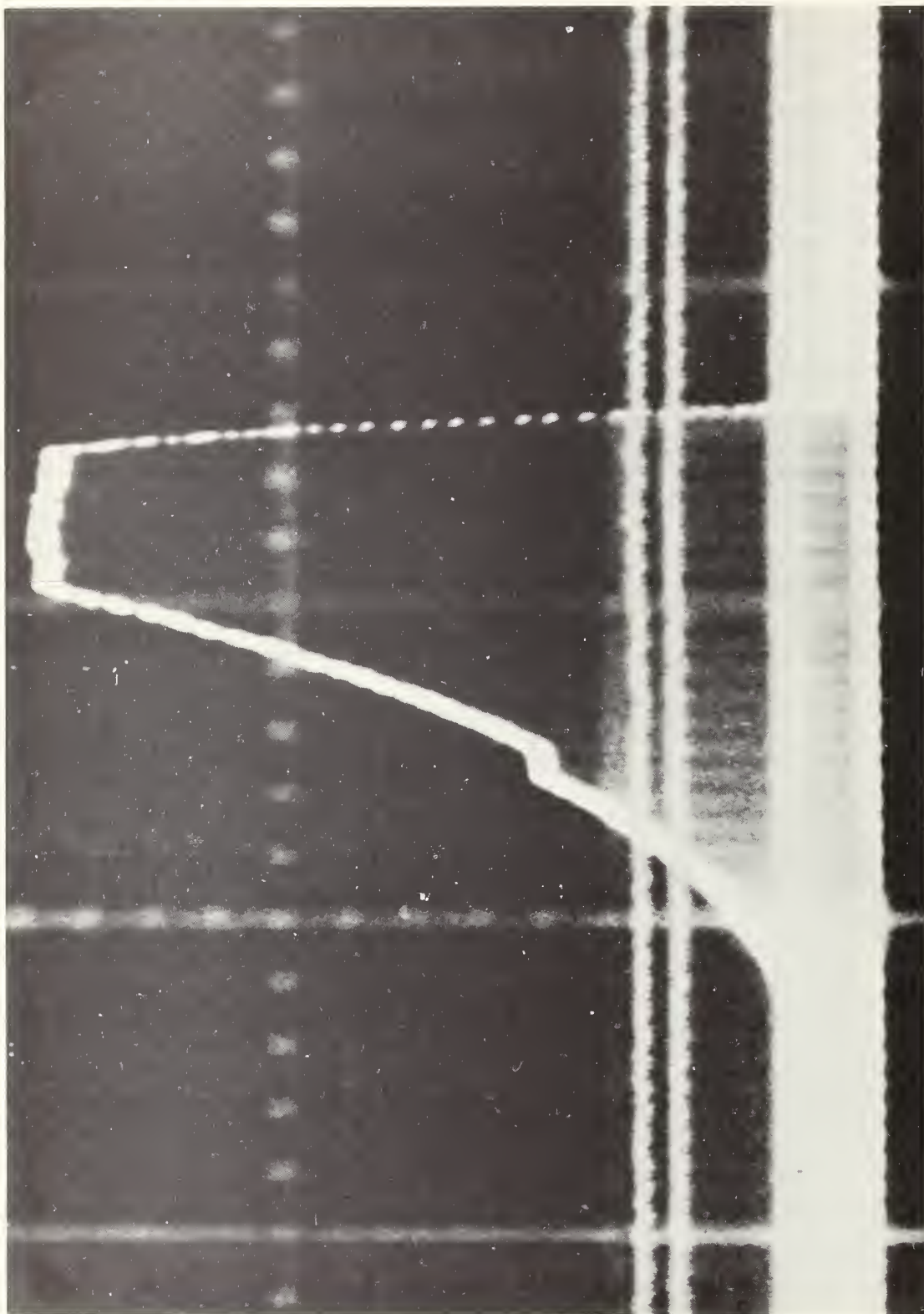
TIME, |—200 ms—|

FIGURE 1   An oscilloscope trace photograph showing the radiance
of a rod-shape specimen during a heating experiment.

42

An oscilloscope trace photograph, showing the variation of the specimen radiance as a function of time during a typical heating experiment, is presented in figure 1. The transformation is indicated by the plateau on the left. The higher plateau on the right indicates melting of the specimen.

Preliminary work had indicated that the abrupt volume changes that occur at the $\alpha \to \gamma$ and the $\gamma \to \delta$ transformations distort the specimen to such an extent that multiple heatings through the transformation region become undesirable. For this reason, in most experiments the specimen was heated from room temperature through the transformation point to its melting point.

Two successive heatings were attempted on two tube-shape specimens, T-1 (Ferrovac E) and T-5 (SRM 734). The attempt on T-1 was not successful. Two successful heatings were conducted on T-5; a low range experiment to 1710 K and a high range experiment to melting. Figure 2 shows the two heating curves for this specimen. The temperature plateau at approximately 1683 K is due to the solid-solid transformation. The higher temperature plateau on the right corresponds to melting of the specimen. A typical heating curve for a rod-shape specimen is shown in figure 3.

The duration of the current pulses in the experiments on tube-shape specimens ranged from 500 to 900 ms while that in the experiments on rod-shape specimens ranged from 800 to 1900 ms. All the experiments were conducted with the specimen in a vacuum environment of approximately 10^{-5} torr.
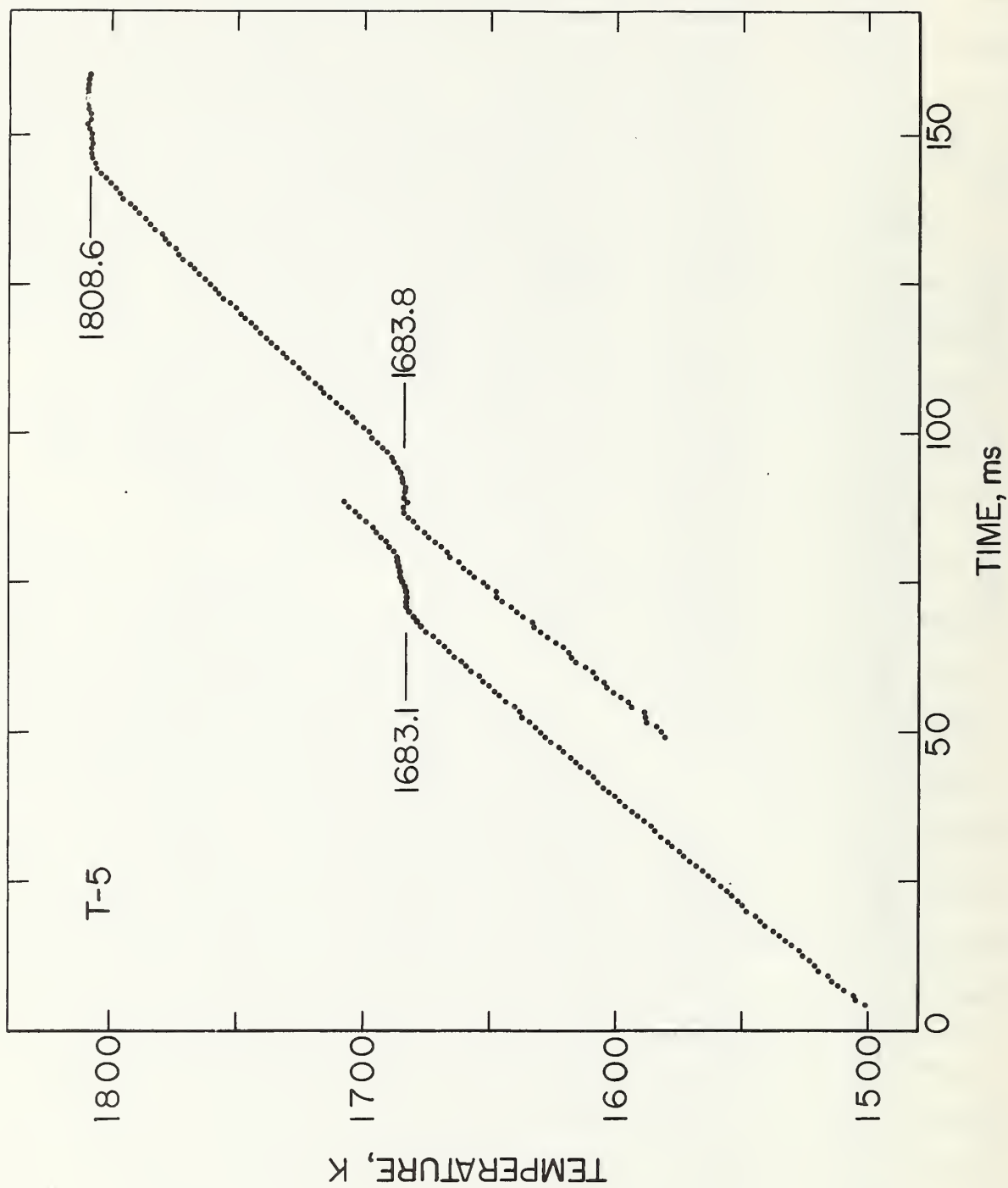
FIGURE 2 Heating curves showing the solid-solid phase transformation ($\gamma \rightarrow \delta$) in iron for a tube-shape specimen.

44

FIGURE 3   Heating curve showing the solid-solid phase transformation

$(\gamma \rightarrow \delta)$ in iron for a rod specimen.

45

4. Results

All the results reported in this paper are based on the International Practical Temperature Scale of 1968 [4].

The measured temperatures in the transformation region are shown in figures 4 and 5 for the tube-shape specimens and in figures 6 and 7 for the rod-shape specimens. Most of the results show an overshoot of approximately 2-5 K at the beginning of the plateau. For each experiment, an average transformation temperature was obtained by averaging the temperatures at the plateau. The results are presented in tables 3 and 4 for tube- and rod-shape specimens, respectively. In the same tables heating rate of the specimens and the maximum deviation of an individual temperature from the average are also given.

Average $\gamma \to \delta$ transformation temperature obtained from measurements on tube-shape specimens are: 1673 K for Ferrovac E iron and 1683 K for SRM 734 iron. Average radiance temperature* at the transformation point obtained from measurements on rod-shape specimens are: 1555 K for Ferrovac E iron and 1562 K for SRM 734 iron. The results of individual experiments are shown, in graphical form, in figure 8.

---

*radiance temperature (sometimes referred to as brightness temperature) is the apparent temperature of the specimen surface as measured by the pyrometer. In order to obtain specimen true temperature normal spectral emittance of the specimen surface at the pyrometer wavelength is required.

46
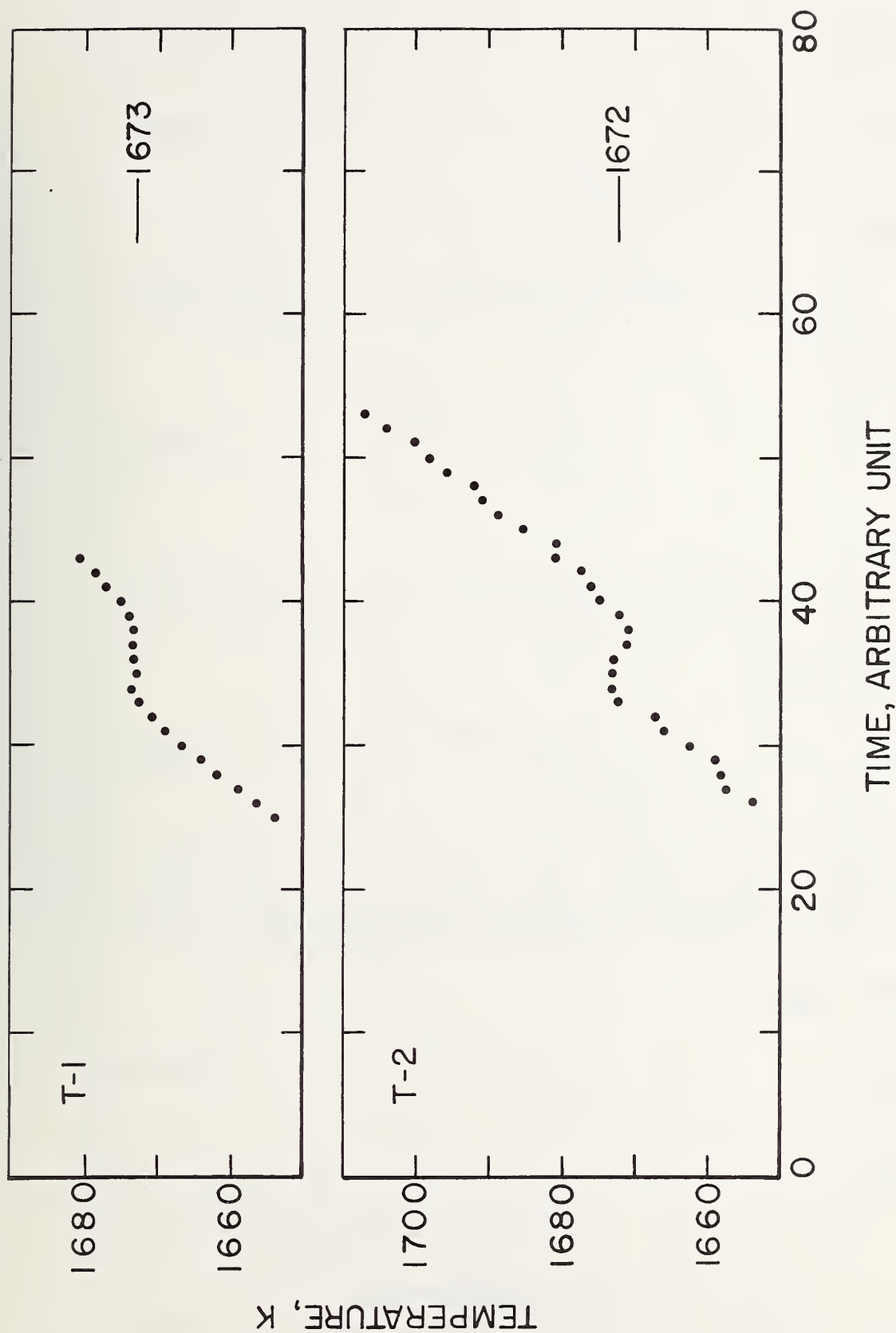
FIGURE 4   Heating curves for the tube-shape specimens of Ferrovac

E iron during the $\gamma \rightarrow \delta$ transformation (one time unit = 0.833 ms).

47
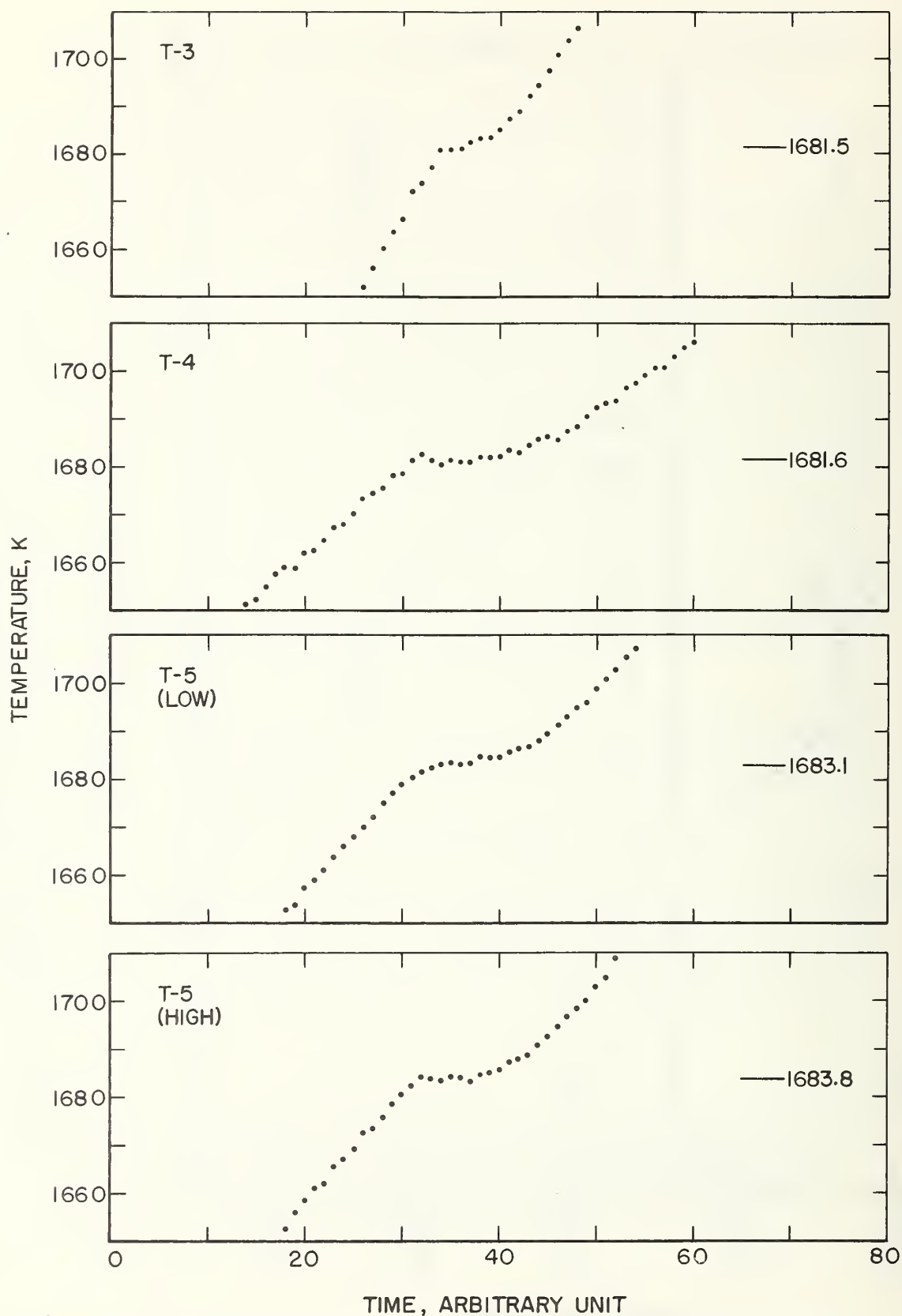
FIGURE 5   Heating curves for the tube-shape specimens of SRM 734

iron during the $\gamma \rightarrow \delta$ transformation. (one time unit = 0.833 ms).

48
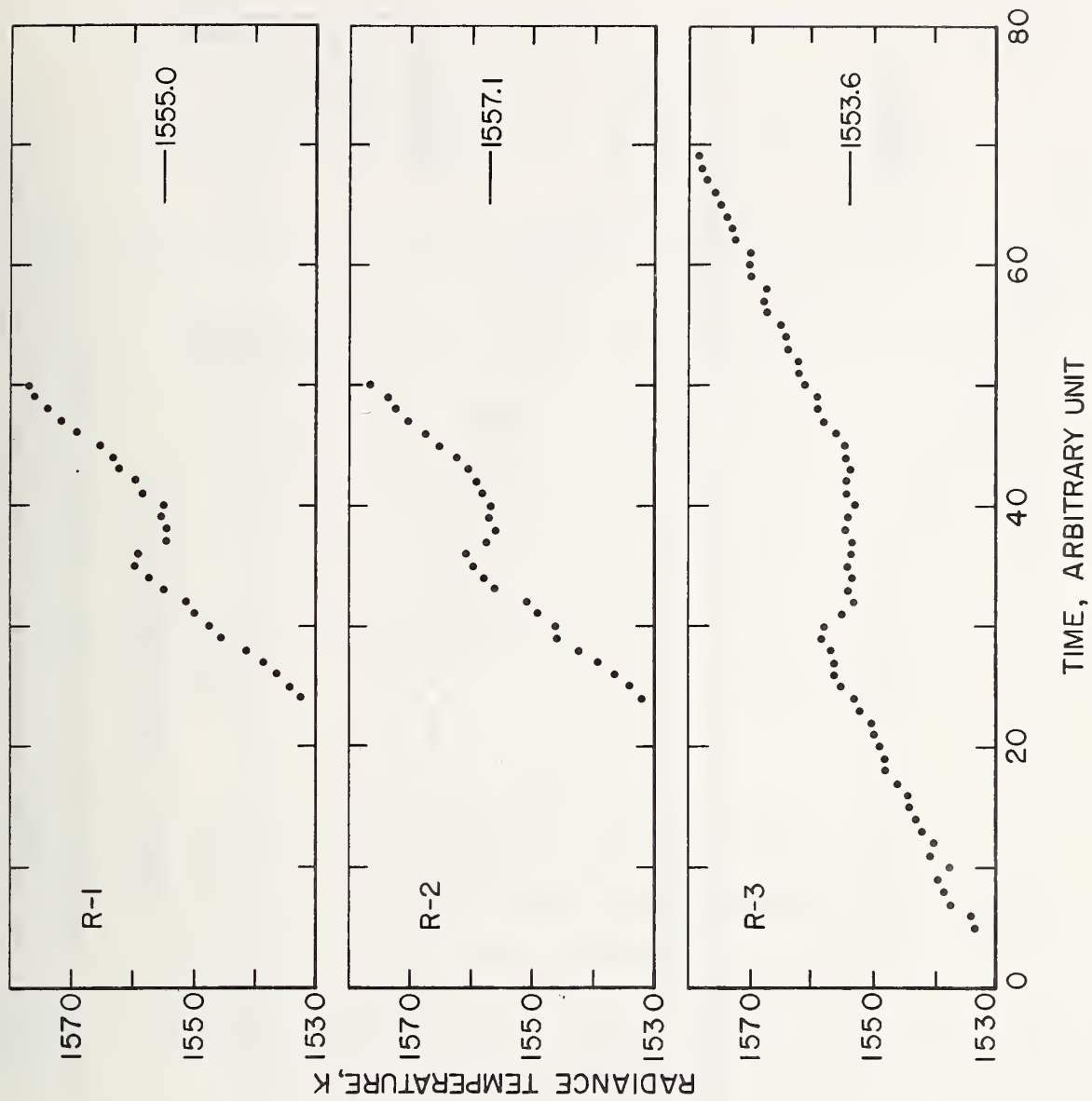
FIGURE 6   Heating curves for the rod-shape specimens of Ferrovac

E iron during the $\gamma \rightarrow \delta$ transformation (one time unit = 0.833 ms).

49
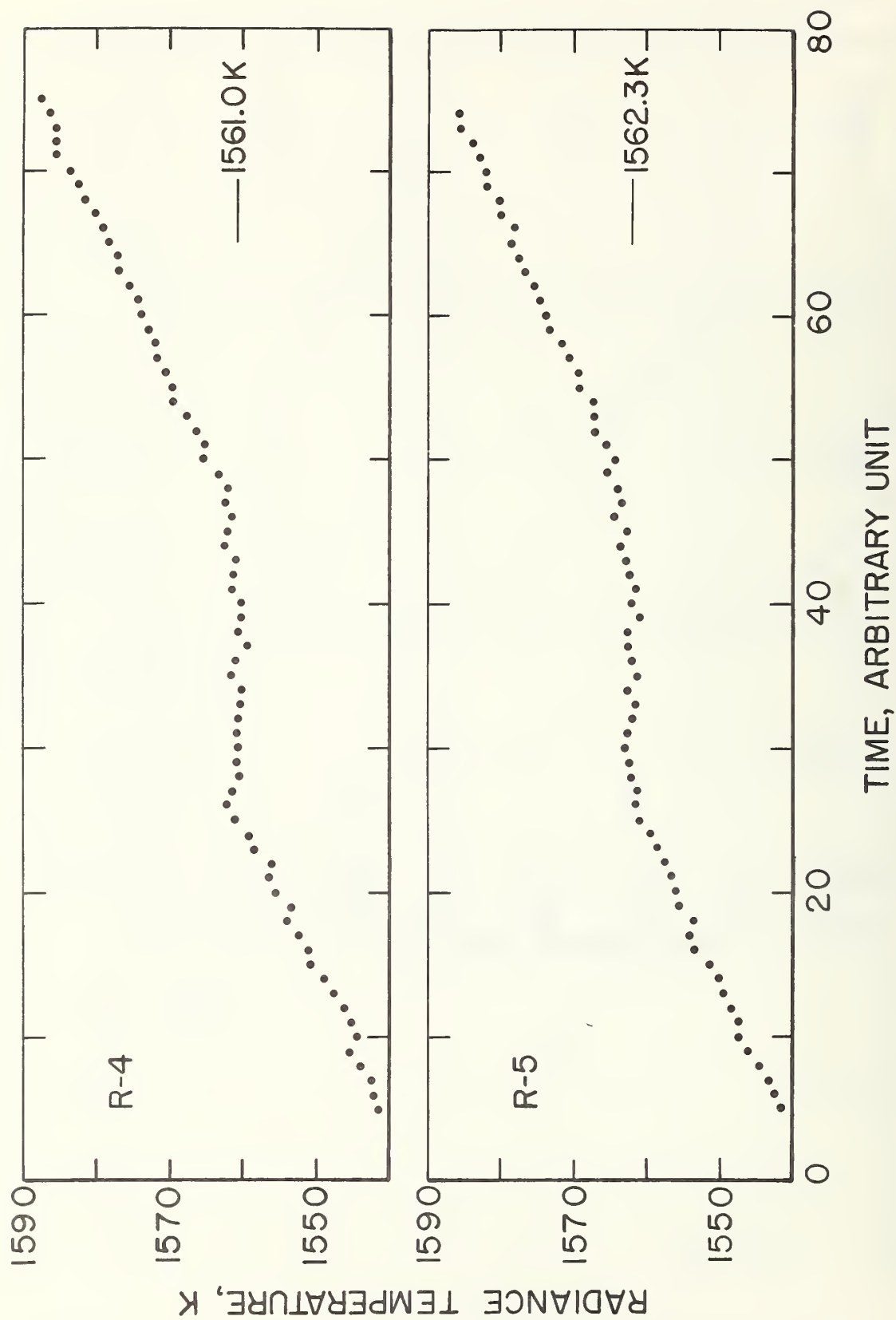
FIGURE 7   Heating curves for the rod-shape specimens of SRM 734

iron during the $\gamma \rightarrow \delta$ transformation.   (one time unit = 0.833 ms).

Table 3

$\gamma \to \delta$

Average transformation temperature and heating

rate just before transformation for the tube-shape iron specimens

Specimen	Type	Avg. Transf. Temp., K	Max. Dev. from Average, K	Heating Rate $K \cdot s^{-1}$
T-1	Ferrovac E	1673.4	0.5	3200
T-2	Ferrovac E	1672.1	1.2	3350
T-3	SRM-734	1681.5	1.2	3000
T-4	SRM-734	1681.6	1.1	2220
T-5 (low)	SRM-734	1683.1	0.5	2630
T-5 (high)	SRM-734	1683.8	0.5	2810

Table 4

Average radiance temperature at the $\gamma \to \delta$ transformation

point, heating rate just before transformation, and average radiance temperature

at the melting point for the rod-shape iron specimens

Specimen	Type	Avg. Rad. Temp. at Transf., K	Max. Dev. from Average, K	Heating Rate $K \cdot s^{-1}$	Avg.Rad.Temp. at Melt., K
R-1	Ferrovac E	1555.0	0.5	2800	1667.2
R-2	Ferrovac E	1557.1	1.1	3190	1666.9
R-3	Ferrovac E	1553.6	1.0	1270	1667.3
R-4	SRM 734	1561.0	1.4	1200	1667.4
R-5	SRM 734	1562.3	1.6	1180	1666.6
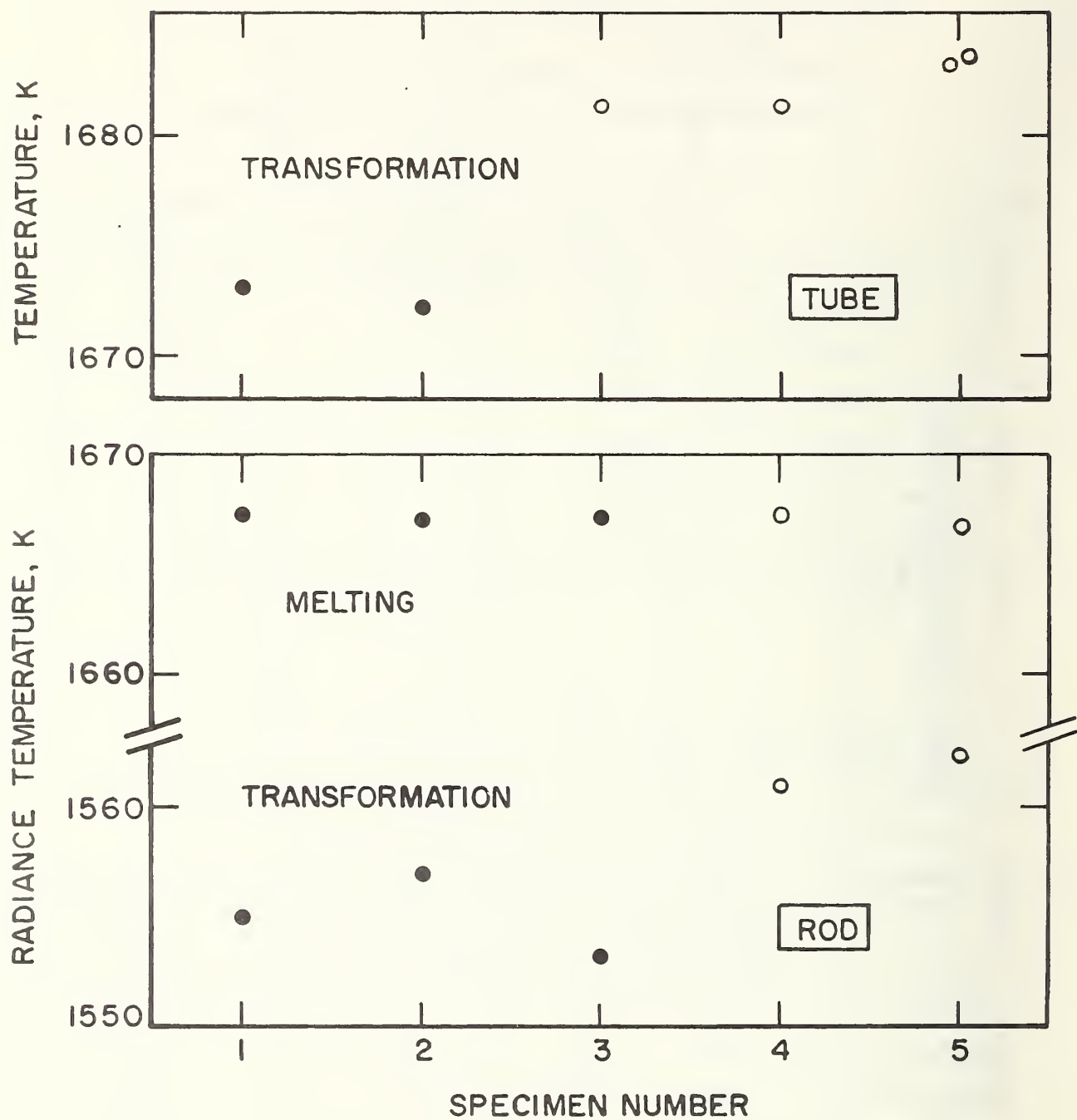
FIGURE 8   Measured radiance temperatures at the transformation

and the melting points and measured temperatures at the

transformation point of iron. (●) Ferrovac E ,(o) SRM 734.

The radiance temperature at the melting point for the rod-shape specimens was also measured. The results on five specimens (table 4) yield an average value of 1667 K for the radiance temperature at the melting point of iron. The maximum difference of an individual result from the average is 0.4 K.

An attempt was made to determine the energy of the transformation from the data taken on the rod-shape specimen (R-4). From the temperature profile around the transformation point, the duration of transformation was obtained. Integration of the power absorbed by the specimen over the transformation period yielded the transformation energy, 890 $J \cdot mol^{-1}$.

The radiance temperature corresponding to the transformation and melting points for the rod-shape specimens in conjunction with similar data on the tube-shape specimens were used to determine the normal spectral emittance at the transformation and the melting points. The melting point of iron was taken as 1808 K [5]. The results of normal spectral emittance are given in table 5 and correspond to 650 nm (the effective wavelength of the high-speed pyrometer with a bandwith of 10 nm). The average values of the normal spectral emittance are: 0.355 at the melting point, and 0.361 and 0.368 at the transformation points for Ferrovac E and SRM 734 irons, respectively.

Table 5

Normal spectral emittance (at 650 nm) of iron at the $\gamma \rightarrow \delta$ transformation

point and at the melting point

Specimen	Type	Normal spectral emittance at transformation point	Normal spectral emittance at melting point
R-1 .	Ferrovac E	0.367	0.356
R-2	Ferrovac E	0.374	0.355
R-3	Ferrovac E	0.362	0.356
R-4	SRM-734	0.359	0.356
R-5	SRM-734	0.363	0.354

Table 6

Temperature and energy of the $\gamma \rightarrow \delta$ transformation

in iron as reported in the literature[*]

Investigator	Ref.	Year	Transf. Temp. K	Transf. Energy $J \cdot mol^{-1}$
Bristow	6	1939	1663	-
Boulanger	7	1956	1667	-
Pattison and Willows	8	1956	1675	870
Olette and Ferrier	9	1958	1675	1170
Ferrier and Olette	10	1962	-	1100
Dench and Kubaschewski	11	1963	1666	837
Braun and Kohlhass	12	1965	-	850

[*] All temperatures are corrected to IPTS 1968.

A detail analysis of errors in such experimental quantities as temperature, voltage and current measured using the present pulse heating system has been given in an earlier publication [3]. The errors in the final results depend on the errors in the experimental quantities as well as on the errors in the method of determining the results from the experimental data. The estimates of sources and magnitudes of the above errors yield the following errors in the reported results: 10 K in transformation temperature, 5 K in radiance temperature, 10% in transformation energy, and 3 and 5% in normal spectral emittance at the melting point and transformation point respectively.

5. Discussion

Experiments on both tubes and rods indicate that the transformation during heating occurs at a lower temperature in Ferrovac E iron *than in* SRM 734 iron (figure 8). The reason for this effect is no*t* known, but it may be due to the relative composition and nature of the impurities in each type of iron. The $\gamma \rightarrow \delta$ transformation temperature reported in the literature is given in table 6. The maximum disagreement in these values is 12 K. The value obtained for Ferrovac E iron is in good agreement (within 2 K) with the values reported by Pattison and Willows [8], and Olette and Ferrier [9]. The value obtained for SRM 734 is 6 to 18 K higher than values reported by other investigators.

The results reported in table 4 for the Ferrovac E rods seem to indicate that the transformation temperature increases with the specimen heating rate. This point was not studied in detail, but it is possible that the heating rate would have some effect on the transformation temperature. A comparison of the experiments on tubes (T-3 and T-4) do not indicate any heating rate effect. The results of figure 5 show that the degree of overshoot at the beginning of the transformation may be dependent on the heating rate. As it may be seen from table 6, considerable disagreements (up to 30%) exist in the values of transformation energy reported in the literature. The closest agreement (within 3%) of the present value is with that reported by Pattison and Willows [8].

The literature contains only a few results on normal spectral emittance of iron at the temperatures reported here. Bidwell [13] has reported a value of 0.38 at the melting point of iron and Burgess and Waltenberg [14] have reported a value of 0.360 at about 1800 K. Near the transformation point the Burgess and Waltenberg have reported a value of 0.370. The results of Wahlin & Knop [15] show an increase of approximately 4.5% in the normal spectral emittance during the transformation. At 1675 K this increase would correspond to an increase in radiance temperature of approximately 6 K. Such as increase is not evident in figures 6 and 7.

56

The experimental results obtained in this work demonstrate the feasibility of using the pulse heating technique to study solid-solid phase transformations in electrical conductors at high temperatures. The results indicate that with proper selection of heating rates and refinements in time resolution, transformation temperatures and energies may be accurately determined and in addition useful information regarding transformation kinetics may be obtained.

Acknowledgement

6. <u>References</u>

[1]   A. Cezairliyan, Design and operational characteristics of
      a high-speed (millisecond) system for the measurement of
      thermophysical properties at high temperatures, J. Res.
      Nat. Bur. Stand. (U. S.), 1971, vol. 75C, (Eng. and Instr.),
      pp. 7-18.

[2]   G. M. Foley, High-speed optical pyrometer, Rev. Sci. Instr.,
      1970, vol. 41, pp. 827-834.

[3]   A. Cezairliyan, M. S. Morse, H. A. Berman, and C. W.,
      Beckett, High-speed (subsecond) measurement of heat capacity,
      electrical resistivity, and thermal radiation properties
      of molybdenum in the range 1900 to 2800 K, J. Res. Nat. Bur.
      Stand. (U. S.), 1970, vol. 74A, (Phys. and Chem.), pp. 65-92.

[4]   International Practical Temperature Scale of 1968, Metrologia,
      1969, vol. 5, pp. 35-44.
                            and
[5]   A. Cezairliyan, J. L. McClure, Thermophysical measurements
      on iron above 1500 K using a transient (subsecond) technique,
      J. Res. Nat. Bur. Stand. (U. S.), Section A, in press.

[6]   C. A. Bristow, Iron Steel Inst. Spec. Rep., No. 24, 1939,
      pp. 1-8.

[7]   C. Boulanger, Contribution à l'étude de la purification
      du fer et à la détermination de ses points de transformation,
      Rev. Metallurg., 1956, vol. 53, pp. 311-319.

[8]   J. R.   Pattison, and P. W.   Willows, The enthalpy of pure
        iron, J. Iron Steel Inst. (London), 1956, vol. 183, pp. 390-403.

[9]   M.   Olette, and A.   Ferrier, High temperature enthalpy of
        gamma and delta pure iron, NPL Symposium, 1958, No. 9, Vol. 2,
        Paper 4H.

[10]   A.   Ferrier, and M.   Olette, Measure de la capacité   calorifique
        du fer entre 910 et 1937°C, Compt. Rend., 1962, vol. 254,
        pp. 2322-2324.

[11]   W. A.   Dench, and W.   Kubaschewski, Heat capacity of iron at
        800°C to 1420°C, J. Iron Steel Inst. (London), 1963, vol. 201,
        pp. 140-143.

[12]   M.   Braun, and R.   Kohlhass, Die spezifische Wärme von
        Eisen, Kobalt und Nickel im Bereich hoher Temperaturen, Phys.
        Stat. Sol., 1965, vol. 12, pp. 429-444.

[13]   C. C.   Bidwell, Radiation from solid and molten iron, Phys.
        Rev., 1913, vol. 1, pp. 482- 483.

[14]   G. K.   Burgess, and R. G.   Waltenberg, The emissivity of
        metals and oxides, Nat. Bur. Std. Bull., 1915, vol. 11,
        pp. 591- 605.

[15]   H. B.   Wahlin, and H. W.   Knop Jr., The spectral emissivity
        of iron and cobalt, Phys. Rev. 1948, vol. 74, pp. 687-689.

Chapter 4

MEASUREMENT OF MELTING POINT, NORMAL SPECTRAL EMITTANCE (AT MELTING POINT) AND ELECTRICAL RESISTIVITY (NEAR MELTING POINT) OF SOME REFRACTORY ALLOYS*

Ared Cezairliyan

Institute for Materials Research

National Bureau of Standards

Washington, D. C. 20234

Abstract

A   subsecond duration pulse heating method is used to measure the melting point, normal spectral emittance (at the melting point, corresponding to 650 nm), and electrical resistivity (near the melting point) of the following refractory alloys: 90 Ta-10W, 99 Nb-1Zr, and 80 Nb-10Ta-10W (numbers indicate nominal composition in percentage by weight). The melting point and the normal spectral emittance are: 3286 ± 15 K and 0.396 for 90Ta-10W, 2737 ± 10 K and 0.351 for 99Nb-1Zr, and 2814 ± 10 K and 0.333 for 80Nb-10Ta-10W. The inaccuracy of the normal spectral emittance and electrical resistivity results is estimated to be 3% and 0.5%, respectively.

---

1. Introduction

A millisecond resolution pulse heating technique was used earlier for the measurement of the melting point, normal spectral emittance (at the melting point), and electrical resistivity (near the melting point) of niobium [1][1]. In the present study, the same technique is used for similar measurements on the refractory alloys: 90Ta-10W, 99Nb-1Zr, and 80Nb-10Ta-10W (numbers indicate nominal composition in percentage by weight).

The technique is based on resistive self-heating of the specimen from room temperature to its melting point in less than one second and measuring current through the specimen, potential difference across the specimen, and specimen temperature. These quantities are measured and recorded digitally every 0.4 ms with a full-scale signal resolution of approximately 1 part in 8000. The details regarding the construction and operational characteristics of the measurement system is given in an earlier publication [2].

2. Measurements

Melting point and electrical resistivity measurements were performed on specimens in the form of tubes having the following nominal dimensions: length, 102 mm; outside diameter, 6.3 mm; and thickness, 0.5 mm. A small rectangular hole (0.5 x 1 mm) fabricated

---

[1]Figures in brackets indicate the literature references at the end of this paper.

in the wall at the middle of the specimen approximated blackbody
conditions for temperature measurements. Normal spectral emittance
measurements were performed on specimens in the form of rods having
the following nominal dimensions: length 76 mm; diameter, 3.1 mm.
The surfaces of all specimens were polished. The composition of
the alloys is given in table 1.

Before starting the experiments, the specimens were heat treated
by subjecting them to 30 heating pulses in the temperature range
2200 to 3000 K. The experiments were conducted in a vacuum
environment of 10^{-4} to 10^{-5} torr. Duration of current pulses
(duration for the specimen to heat from room temperature to its
melting point) was in the range 380 to 750 ms.

For each alloy two experiments were performed for the
determination of the melting point and one experiment was performed
for the determination of normal spectral emittance and electrical
resistivity. Designation of the specimens and the results of
some of the measurements are given in table 2. All measurements
reported in this paper are based on the International Practical
Temperature Scale of 1968 [3].

Table 1   Composition of the alloys

Alloy	Major Constituents (% by weight)	Total Impurities (% by weight)
90Ta-10W	Ta, 90.45; W, 9.45	0.10
99Nb-1Zr	Nb, 98.78; Zr, 1.05	0.17
80Nb-10Ta-10W	Nb, 80.94; Ta, 9.70; W, 9.30	0.06

Table 2

Specimen designations and the results of individual experiments

Specimen Number	Substance	Geometry	Pulse Length (ms)	Melting Point			Radiance Temp. at melting point		
				Number of Temp.	Melting Point(K)	Stand. Dev.	Number of Temp.	Rad. Temp.(K)	Stand. Dev.
1	90 Ta-10 W	tube	480	12	3287.0	1.3			
2	90 Ta-10 W	tube	750	15	3285.12	0.8			
3	90 Ta-10 W	rod	600				26	2888.7	0.4
4	99 Nb-1 Zr	tube	380	23	2737.0	1.9			
5	99 Nb-1 Zr	tube	390	24	2737.6	1.3			
6	99 Nb-1 Zr	rod	380				21	2423.2	0.8
7	80 Nb- 10 Ta-10 W	tube	630	21	2816.1	0.3			
8	80 Nb- 10 Ta-10 W	tube	660	30	2812.8	0.6			
9	80 Nb- 10 Ta-10 W	rod	610				8	2469.2	0.2

2.1. Melting Point

Temperature of the tubular specimens was measured near and during the initial melting period. A plateau in temperature indicated the transition from solid to liquid phase. Measured temperatures at the plateau for specimens are shown in figure 1. The melting point for each specimen was obtained by averaging the temperature points on the plateau. The results are presented in table 2. The standard deviation of an individual point was in the range 0.3 to 1.9 K. As may be seen in table 2, the difference between the results for the two specimens of the same alloy was in the range 0.6 to 3.3 K. The average melting points of the alloys are given in table 3.

2.2. Normal Spectral Emittance

Normal spectral emittance at the melting point of each alloy was determined from the measurements of the radiance temperature of the specimen (in rod form) and the average melting point obtained from the measurements on the tubular specimens. Based on the Wien radiation equation, the relation between emittance and temperature is

$$\epsilon = \frac{1}{\exp[\frac{c_2}{\lambda}(\frac{1}{T_s} - \frac{1}{T_m})]}$$

where ϵ is the normal spectral emittance, T_m the melting point, T_s the radiance temperature, c_2 the second radiation constant (1.4388 × 10^{-2} m K), and λ the effective wavelength of the optical

64

Table 3

Melting point (T_m), radiance temperature (T_s) at the melting point, and normal spectral emittance (ϵ) at the melting point of some refractory alloys

Substance	T_m(K)	T_s(K) (at 650 nm)	ϵ (at 650 nm)
90 Ta - 10 W	3286	2889	0.396
99 Nb - 1 Zr	2737	2423	0.351
80 Nb - 10 Ta - 10 W	2814	2469	0.333
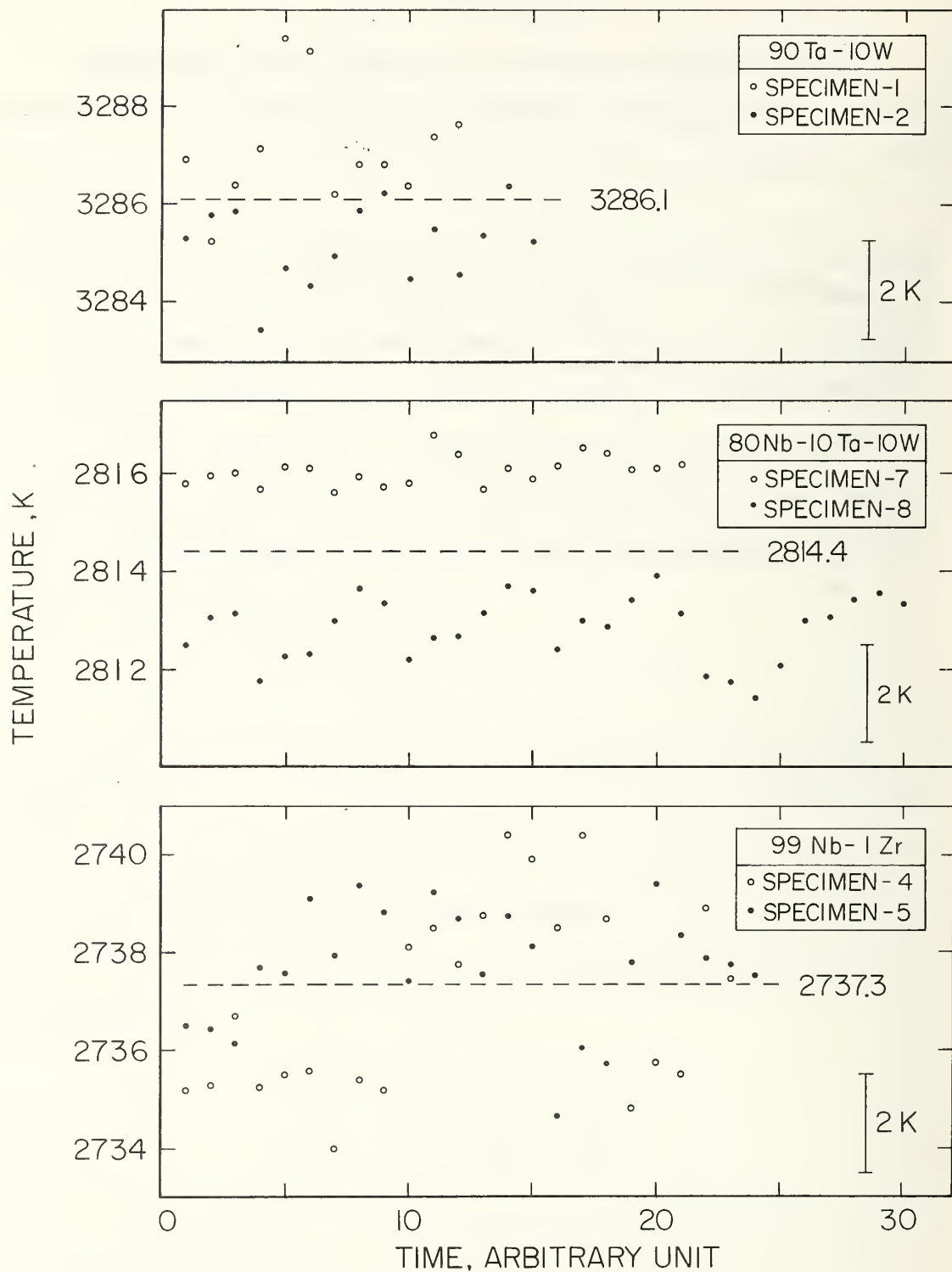
FIGURE 1. Variation of the temperature of various refractory
alloys as a function of time at their respective
melting points (1 time unit = 0.833 ms).

66

system. The measurements were performed at 650 nm which corresponds to the effective wavelength of the pyrometer's interference filter. The bandwith of the filter was 10 nm. The circular area viewed by the pyrometer was 0.2 mm in diameter.

The experimental results of the radiance temperature of 90Ta-10W and 99Nb-1Zr alloys near and at the respective melting points are shown in figure 2. Similar results for the alloy 80Nb-10Ta-10W are shown in figure 3. It may be seen (figure 2) that both 90Ta-10W and 99Nb-1Zr samples behaved normally, that is, radiance temperature increased and exhibited a plateau upon melting. However, 80Nb-10Ta-10W results (figure 3) do not indicate the existence any well-defined plateau, with the exception of a short segment immediately after reaching the melting point. The results of radiance temperature at the melting point of the alloys and corresponding values for the normal spectral emittance are given in table 3.

2.3. Electrical Resistivity

Electrical resistivity of the tubular specimens was calculated using the relation ρ = RA/L, where R is the resistance, A the cross-section area, and L the length of the specimen between the potential probes. The dimensions were based on their room temperature values; the cross-section al area was determined from the measurement of weight and density. The results for the electrical resistivity of the alloys near and at their respective melting points are shown in figures 4,
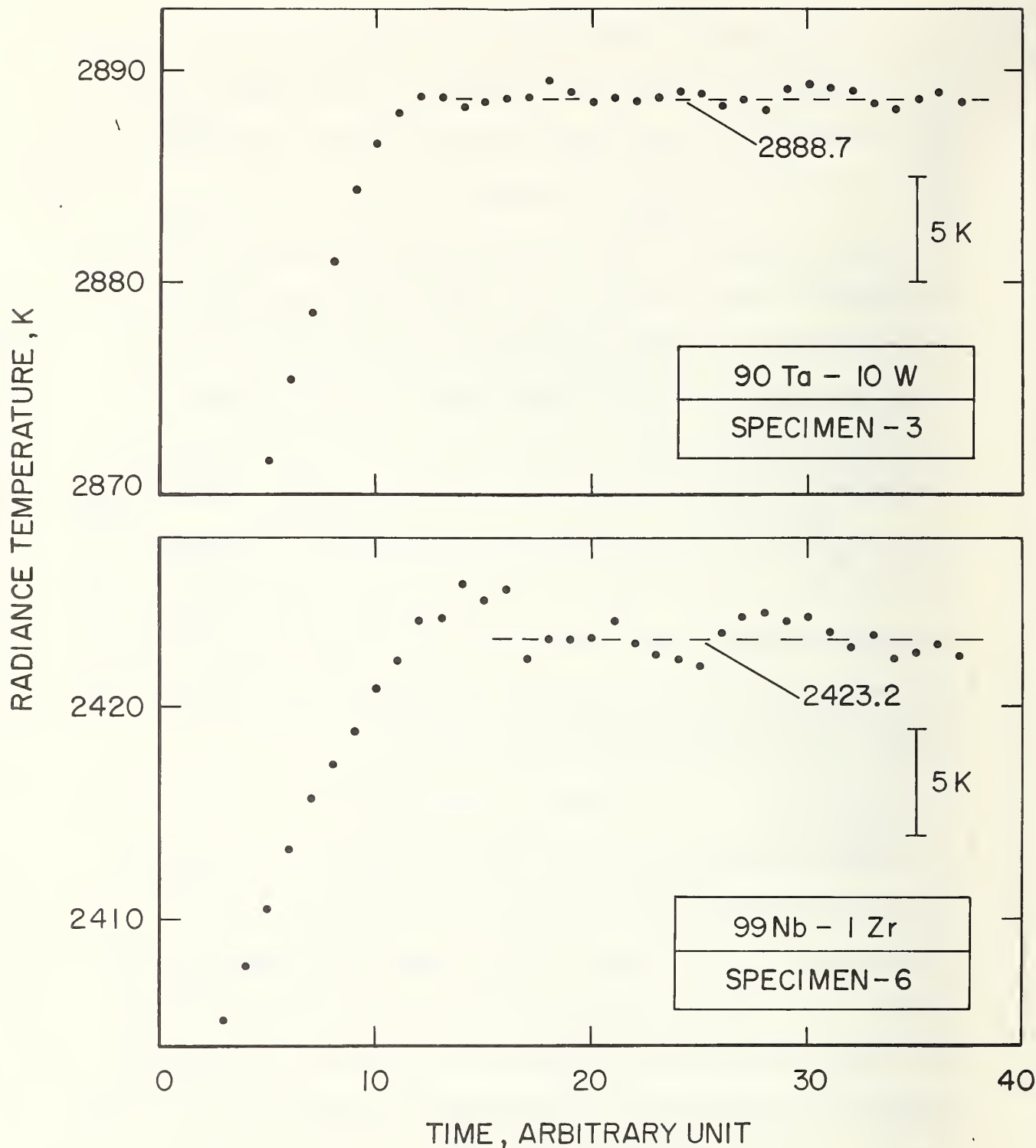
FIGURE 2.   Variation of the radiance temperature (at 650 nm) of
the alloys 90 Ta - 10 W and 99 Nb-1 Zr as a function
of time near and at their respective melting points
(1 time unit = 0.833 ms).

68
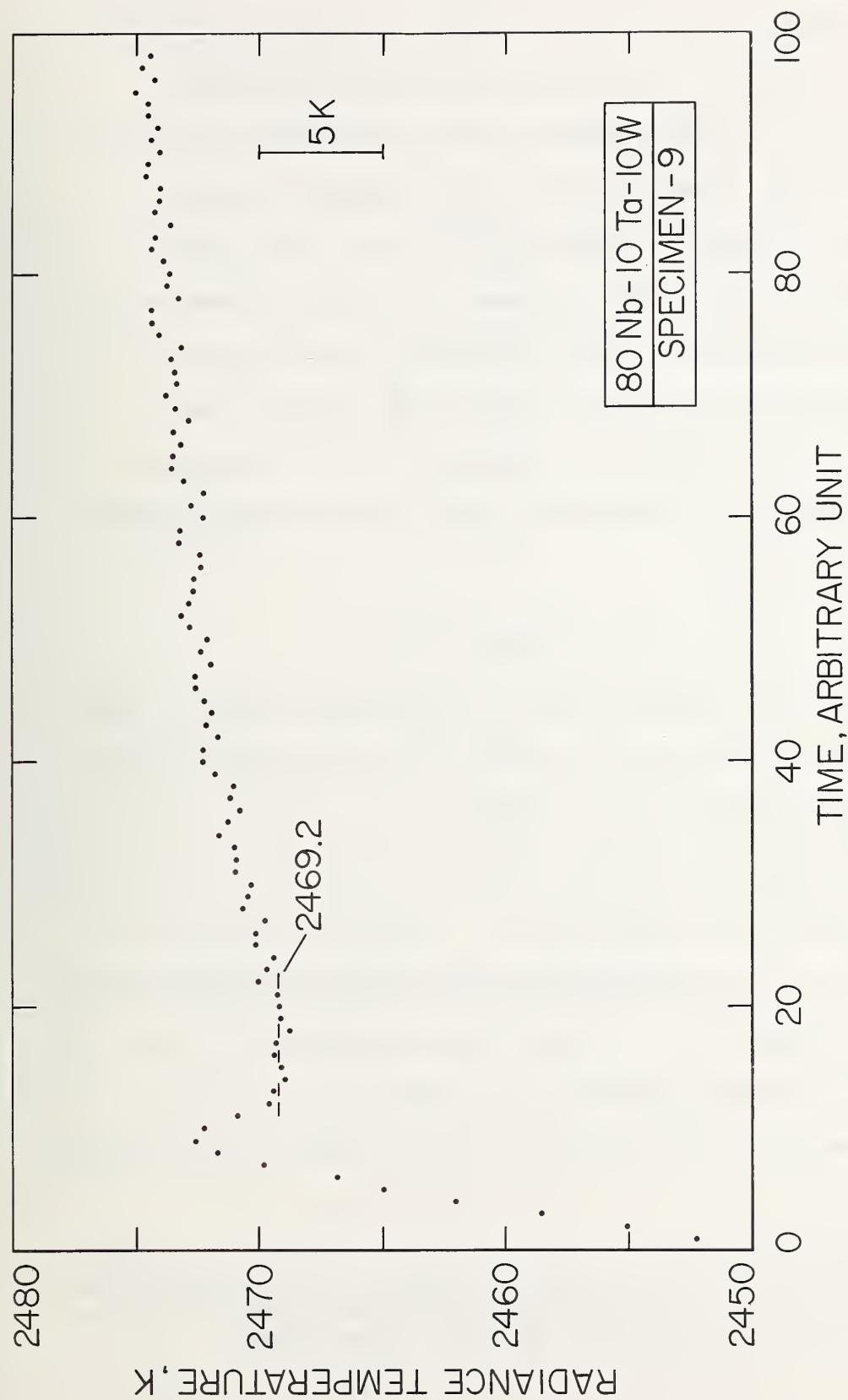
FIGURE 3. Variation of the radiance temperature (at 650 nm) of
the alloy 80 Nb-10 Ta-10 W as a function of time near
and at its melting point (1 time unit = 0.833 ms).

5 and 6. The values for the 100 K range below the melting points are given in table 4. The results indicate that electrical resistivity of the alloys 90Ta-10W (figure 4) and 99Nb-1Zr (figure 5) changed almost abruptly at the start of melting. However, in the case of the alloy 80Nb-10Ta-10W (figure 6) the change in the electrical resistivity was gradual, starting approximately 15 K below the melting point. Below the melting point electrical resistivity for each alloy was fitted, using the least squares method, to a linear function in temperature. In all cases, the standard deviation of an individual point from the smooth function was less than 0.06%.

2.4. Estimate of Errors

Sources and estimates of errors in experiments similar to the ones conducted in this study are given in earlier publications [4, 5]. Specific items in the error analysis were recomputed whenever the present conditions differed from those in the earlier publications.

As it may be seen from table 2, the imprecision[2] of true (blackbody) and radiance temperature measurements was 0.3-1.9 K and 0.2-0.8 K, respectively. A somewhat higher imprecision in the case of the blackbody temperature measurements may be attributed to the movements of the sighting hole in the specimen during melting.

---

[2] Imprecision refers to the standard deviation of an individual point as computed from the difference between measured value and that from the smooth function obtained by the least squares method.

Table 4

Electrical resistivity of some refractory

alloys near their melting points

Alloy	Temp. (K)	Elec. Res.[*] (10^{-8} Ω m)
90 Ta - 10 W	3180	110.88
	3230	112.03
	3280	113.17
99 Nb - 1 Zr	2630	87.06
	2680	88.25
	2730	89.43
80 Nb - 10 Ta - 10 W	2700	88.49
	2750	89.70
	2800	90.92

[*]Based on ambient temperature (298 K) dimensions.
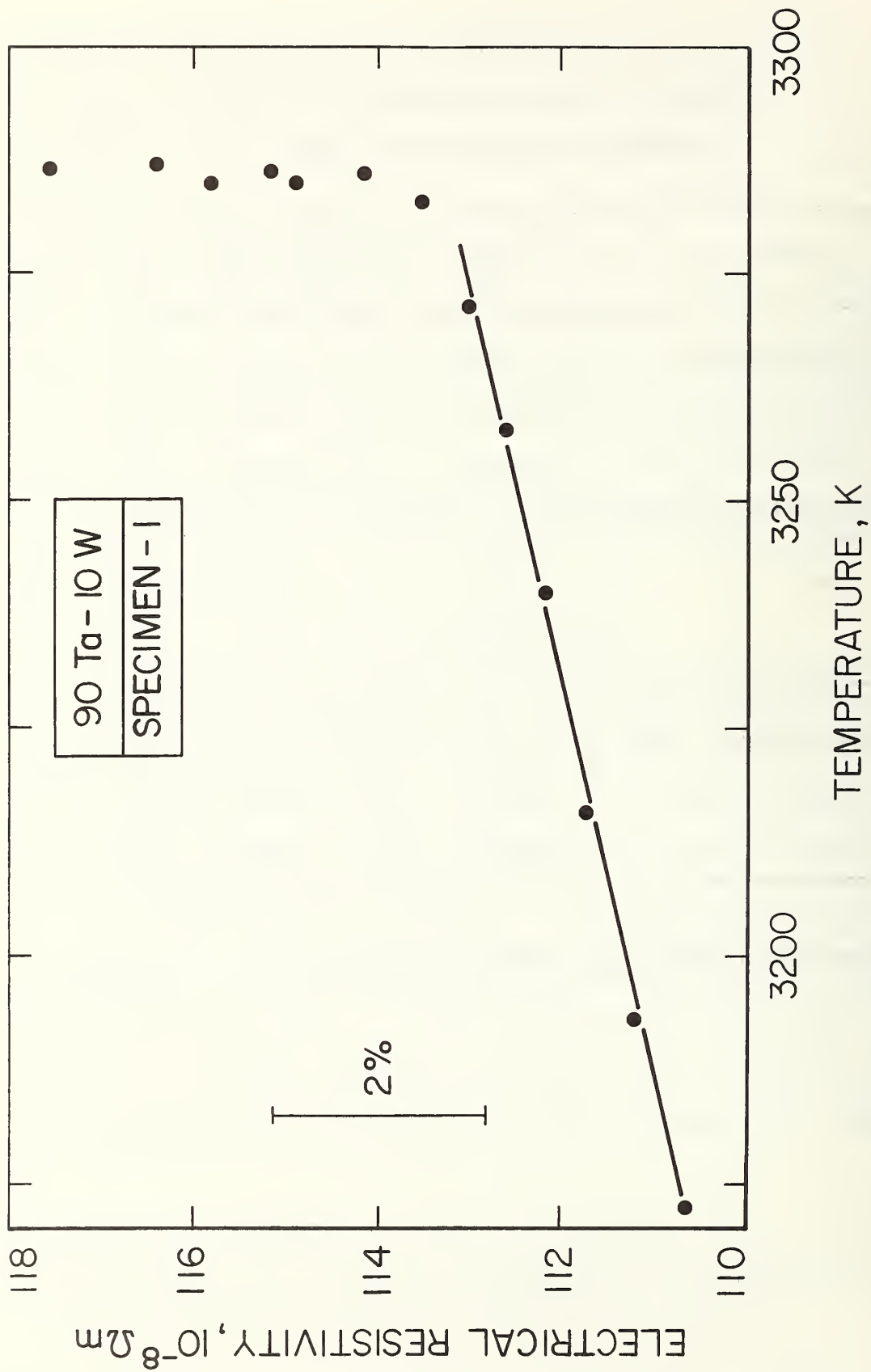
FIGURE 4. Electrical resistivity of the alloy 90 Ta-10 W near and at its melting point.
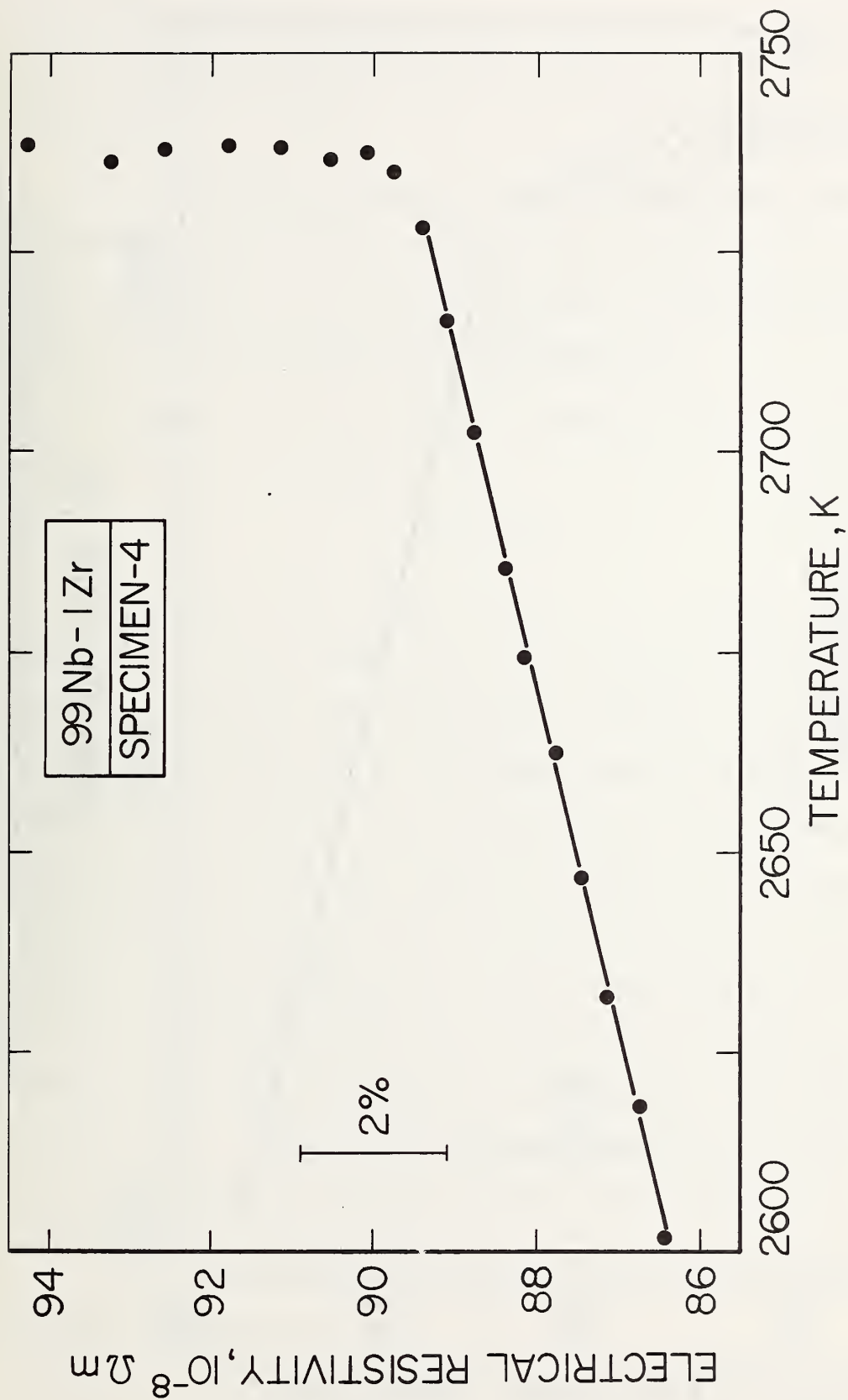
FIGURE 5. Electrical resistivity of the alloy 99 Nb-1 Zr near and at its melting point.
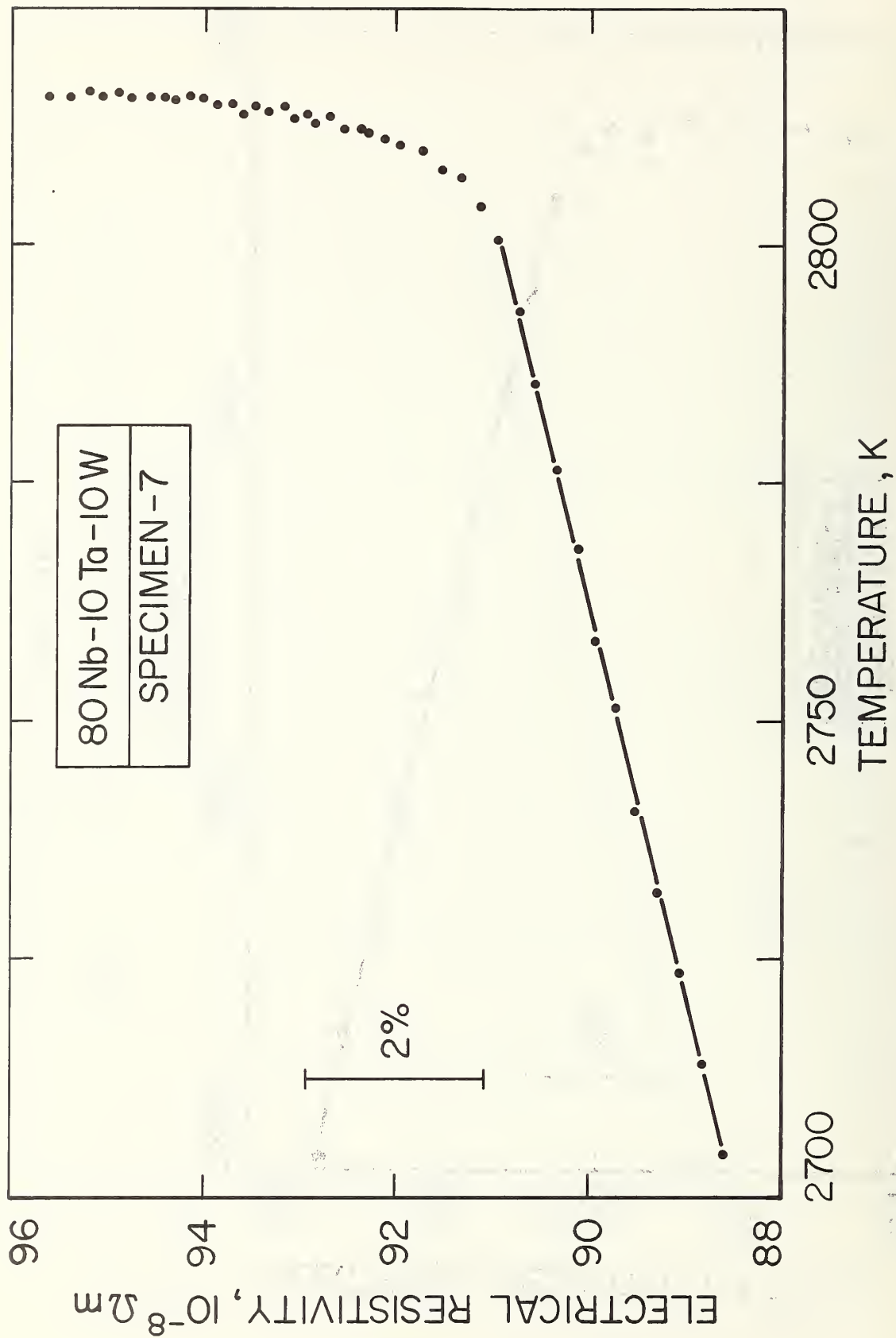
FIGURE 6. Electrical resistivity of the alloy 80 Nb-10 Ta-10 W near and at its melting point.

74

The inaccuracy[3] of the melting points is estimated to be approximately 10 K for the alloys 99Nb-1Zr and 80Nb-10Ta-10W, and 15 K for 90Ta-10W.

The combination of inaccuracies in the temperature measurements, taking into account likely common errors in both blackbody and radiance temperature measurements, indicates that the inaccuracy in the normal spectral emittance is approximately 3%.

The imprecision of the electrical resistivity results is 0.05% and the estimated inaccuracy is 0.5%.

3. Discussion

The agreement of the melting points of the specimens of the same alloy were in the range 0.6 to 3.3 K, indicating reasonably good reproducibility of the measurements. Radiance temperature and electrical resistivity of the binary alloys 90Ta-10W and 99Nb-1Zr behaved normally, that is exhibited an almost abrupt change at the beginning of melting. However, in the case of the ternary alloy 80Nb-10Ta-10W the change in electrical resistivity was more gradual, starting approximately 15 K below the melting point. Radiance temperature of the ternary alloy exhibited a peak before melting, a short plateau immediately after the start of melting, and a continuous increase as melting progressed. The peak may be due to the roughness of the solid surface, and the increase in radiance temperature during melting may be attributed to the increase

---

[3] Inaccuracy refers to the estimated total error (random and systematic).

75

of the normal spectral emittance during melting. With the present
system it was not possible to follow the entire melting process
because the specimens collapsed and opened the electrical circuit
prior to the completion of melting.

.

4. References

[1]   Cezairliyan, A., Measurement of Melting Point, Normal Spectral Emittance (at Melting Point), and Electrical Resistivity (above 2650 K) of Niobium by a Pulse Heating Method, High Temperatures - High Pressures, 4, 453 (1972).

[2]   Cezairliyan, A., Design and Operational Characteristics of a High-Speed (Millisecond) System for the Measurement of Thermophysical Properties at High Temperatures, J. Res. Nat. Bur. Stand. (U. S.), 75C (Eng. and Instr.), 7 (1971).

[3]   International Practical Temperature Scale of 1968, Metrologia, 5, 35 (1969).

[4]   Cezairliyan, A., Morse, M. S., Berman, H. A., and Beckett, C. W., High-Speed (Subsecond) Measurement of Heat Capacity, Electrical Resistivity, and Thermal Radiation Properties of Molybdenum in the Range 1900 to 2800 K, J. Res. Nat. Bur. Stand. (U. S.), 74A (Phys. and Chem.), 65 (1970).

[5]   Cezairliyan, A., Morse, M. S., and Beckett, C. W., Measurement of Melting Point and Electrical Resistivity (Above 2840 K) of Molybdenum by a Pulse Heating Method, Rev. Int. Hautes Tempér. et Réfract., 7, 382 (1970).

THE ENTHALPY OF FORMATION OF $MoF_5(c)$ BY SOLUTION CALORIMETRY:

PRELIMINARY ANALYSIS OF EXPERIMENTS

R. L. Nuttall, M. V. Kilday, and K. L. Churney

1. Introduction

This laboratory is engaged in a program to determine the enthalpy of formation of the lower fluorides of molybdenum. The compound of current interest is $MoF_5(c)$. The method finally selected for determining the enthalpy of formation of $MoF_5(c)$ was to measure the heat of solution of $MoF_5(c)$ in a solution of HF and XeO_3 and of $MoF_6(\ell)$ in a similar solution to give the same concentrations of all the aqueous species in the two final solutions. This method requires an accurate knowledge of the enthalpy of formation of $MoF_6(\ell)$ and XeO_3 (solution).

The enthalpy of formation of $MoF_6(g)$ was measured by Settle et. al. [1] by direct combination of the elements in a combustion bomb. A recalculation of their results [2] combined with the selected value of the heat of vaporization [3] of $MoF_6(\ell)$ gives a value of -1585.53 ± 0.92 kJ mol^{-1} (-378.95 ± 0.22 kcal mol^{-1}) for the enthalpy of formation of $MoF_6(\ell)$.

Previous measurements in our laboratory [4] of the heats of solution of $MoF_6(\ell)$ and $MoO_3(c)$ in basic solution gave a value of $\Delta H_f^\circ[MoF_6(\ell)]$ of -1574.98 ± 2.18 kJ mol^{-1} (-376.43 ± 0.52 kcal mol^{-1}). The assigned uncertainty is due primarily to the total estimated uncertainty of our experimental measurements, ± 2.09 kJ mol^{-1}, and does not include any uncertainty in the value taken for the enthalpy

of formation of F^-(aq) of -332.63 kJ mol^{-1} (-79.50 kcal mol^{-1}) [5].
Using a value of $\Delta H_f^\circ[F^-(aq)]$ of -335.35 ± 0.65 kJ mol^{-1} (-80.15 ±
0.16 kcal mol^{-1}) selected in a more recent critical evaluation [6],
we obtain a value for $\Delta H_f^\circ[MoF_6(\ell)]$ from our previous experimental
measurements of -1591.30 ± 3.72 kJ mol^{-1} (-380.33 ± 0.89 kcal mol^{-1}).
The agreement between the latter and the value derived from the
measurements of Settle et. al. is considered to be satisfactory.

XeO_3(aq) was originally chosen as an oxidizing agent to deter-
mine if a reaction scheme involving basic rather than acidic solution
could be characterized. The negative results of this preliminary
investigation are discussed briefly in the Appendix. In dilute acid
solutions, XeO_3(aq) is stable and forms the single product Xe(g) in
an oxidation-reduction reaction [7,8]. The enthalpy of formation of
$[XeO_3 \cdot 96.15\ H_2O\ (\ell)]$ in a dilute acid solution was determined by
O'Hare, Johnson, and Appelman [7]. They report a value of 418.15 ±
1.00 kJ mol^{-1} (99.94 ± 0.24 kcal mol^{-1}) and a heat of dilution to
$[XeO_3 \cdot 14,000\ H_2O(\ell)]$ of 0 ± 126 J mol^{-1} (0 ± 30 cal mol^{-1}).

2. Reaction Schemes of Solution Experiments

A scheme of reactions that yields the enthalpy of formation of
MoF_5(c) is as follows:

$$MoF_5(c) + [(n_1 + 1/6)XeO_3 + (n_2 - 5)HF + (n_3 + 7/2)H_2O](\text{soln I}) = \quad (1)$$
$$[H_2MoO_4 + n_1XeO_3 + n_2HF + n_3H_2O](\text{soln II}) + 1/6\ Xe(g) - \Delta H_1$$
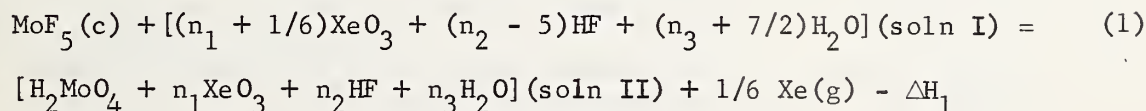
$$\text{MoF}_6(\ell) + [\text{n}_1\text{XeO}_3) + (\text{n}_2 - 6)\text{HF} + (\text{n}_3 + 4)\text{H}_2\text{O}](\text{soln III}) = [\text{II}] - \Delta\text{H}_2 \quad (2)$$

$$[\text{I}] + \infty\text{H}_2\text{O}(\ell) = \quad\quad\quad\quad\quad\quad\quad\quad\quad\quad\quad\quad\quad\quad\quad\quad\quad (3)$$
$$(\text{n}_1 + 1/6)\text{XeO}_3(\text{aq}) + (\text{n}_2 - 5)\text{HF}(\text{aq}) + (\text{n}_3 + 7/2)\text{H}_2\text{O}(\text{aq}) - \Delta\text{H}_3$$

$$[\text{III}] + \infty\text{H}_2\text{O}(\ell) = \text{n}_1\text{XeO}_3(\text{aq}) + (\text{n}_2 - 6)\text{HF}(\text{aq}) + (\text{n}_3 + 4)\text{H}_2\text{O}(\text{aq}) - \Delta\text{H}_4 \quad (4)$$

Adding equations (1) - (2) - (3) + (4) gives

$$\text{MoF}_5(\text{c}) + 1/6\text{XeO}_3(\text{aq}) + \text{HF}(\text{aq}) = \text{MoF}_6(\ell) + 1/2\text{H}_2\text{O}(\ell) + 1/6\text{Xe}(\text{g}) - \Delta\text{H}_5 \quad (5)$$

where ΔH_5 is given by

$$\Delta\text{H}_5 = \Delta\text{H}_1 - \Delta\text{H}_2 - \Delta\text{H}_3 + \Delta\text{H}_4 \quad\quad\quad\quad\quad\quad\quad\quad\quad\quad (6)$$

The heat of formation of $\text{MoF}_5(\text{c})$ is calculated from the expression

$$\Delta\text{H}_f^\circ[\text{MoF}_5(\text{c})] = \Delta\text{H}_f^\circ[\text{MoF}_6(\ell)] + 1/2\Delta\text{H}_f^\circ[\text{H}_2\text{O}(\ell)] - 1/6\Delta\text{H}_f^\circ[\text{XeO}_6(\text{aq})] - \quad (7)$$
$$\Delta\text{H}_f^\circ[\text{HF}(\text{aq})] - \Delta\text{H}_5$$

In this scheme, ΔH_1 and ΔH_2 are measured experimentally. ΔH_3 and ΔH_4 are estimated from literature values [9] of the heat of dilution data for HF solutions and eq. (8).

$$\Delta\text{H}_4 - \Delta\text{H}_3 \cong (\text{n}_2 - 6)(\varphi_L(\frac{\text{n}_3 + 7/2}{\text{n}_2 - 5}) - \varphi_L(\frac{\text{n}_3 + 4}{\text{n}_2 - 6})) + \varphi_L(\frac{\text{n}_3 + 7/2}{\text{n}_2 - 5}) \quad (8)$$

In eq. (8), $\varphi_L(x)$ is the apparent molal enthalpy of HF in a solution with x moles of water. We have assumed there is no interaction between XeO_3 and HF and that the heat of dilution of XeO_3 is zero. Experiments will be carried out to test the validity of these assumptions.

80

3. Experimental

    a. Materials

        MoF$_6$ was purchased from Ozark-Mahoning Company.* It was purified
by trap-to-trap distillation and was then transferred by distillation into
Kel-F (polychlorotrifluoroethylene) bulbs for introduction into the
calorimeter. The sample bulbs have been described previously [4].
Samples of MoF$_6$ which had received similar treatment were analyzed
by freezing point lowering by Krause [10] who found an impurity of
0.03 mol percent. The nature of the impurity was not determined.

        MoF$_5$ was made by reacting MoF$_6$ with molybdenum powder at 150 C.
The MoF$_5$ was then distilled off and purified by trap-to-trap distillation
at 90 C with an atmosphere containing MoF$_6$ at a partial pressure of
about 17 Pa. The light yellow crystalline material was trans-
ferred into the platinum calorimeter sample holder in an atmosphere
of dry Argon.

    b. Calorimeter

        The calorimeter used was a precise adiabatic calorimeter with
an all-platinum interior. Its description and operation are given
elsewhere [11].

4. Results

    a. Experimental Results

        Results of the calorimetric measurements are given in Table 1
for the solution of MoF$_5$ and in Table 2 for the solution of MoF$_6$.
In these tables n_1, n_2, and n_3 are the coefficients in equations (1)

* Disclaimer

and (2). ϵ is the energy equivalent of the calorimeter obtained as the mean of two calibration experiments, one before and one after the reaction experiment. ΔT_c is the corrected temperature rise of the calorimeter. Q is the measured heat of reaction equal to ΔT_c times ϵ. $\bar{T}$ is the average temperature of reaction.

The data analysis given here is preliminary and will be refined at a later time. Based on the data in Table 1, we estimate[*] a heat of reaction (1) of

$$-\Delta H_1 = 340.01 \pm 1.0 \text{ kJ mol}^{-1} \quad (81.26 \pm 0.5 \text{ kcal mol}^{-1})$$

The mass of sample given in Table 2 was determined by weighing the plastic bulb (with its sidearm attached), filling with $MoF_6(\ell)$, sealing by pinching off the sidearm and weighing the filled bulb and then the separated sidearm. An alternate method of determining the sample size is to weigh the filled bulb and then weigh the empty bulb removed from the calorimeter after the reaction. These two procedures give sample weights that differ by milligrams.

Using sample weights determined by the second procedure we estimate values of

$-\Delta H_2$	261.43 kJ mol^{-1}	(62.48 kcal mol^{-1})
Std. dev.	2.65 kJ mol^{-1}	(0.63 kcal mol^{-1})
Std. dev. mean =	0.88 kJ mol^{-1}	(0.21 kcal mol^{-1})

---

[*] The corrections for the vaporization of water by the Xe(g) evolved and the Ar(g) liberated when the sample holder is opened are approximately 0.01% and 0.01-0.03% of ΔH_1, respectively. They are small in comparison to other systematic errors in the final value obtained for $\Delta H_f^\circ[MoF_5(c)]$ and have not been included in these results.

to be compared with the values given in Table 2. We thus have a systematic uncertainty in ΔH_2 of about one kilocalorie per mole. We are now analyzing the final solutions from the calorimetric experiments to obtain a value for the amount of sample used. We expect to be able to reduce the uncertainty in the value of ΔH_2.

We estimate an average value of $-\Delta H_2 = 259.39 \pm 4.$ kJ mol^{-1} $(62.00 \pm 1.$ kcal mol$^{-1})$.

b. Evaluation of $(\Delta H_4 - \Delta H_3)$

Using average values of n_2 and n_3 from Tables 1 and 2 and values of φ_L from Parker [10] we get $n_2 = 20.43$, $n_3 = 14930$.

$$(n_3 + 7/2)/(n_2 - 5) = 968$$

$$(n_3 + 4)/(n_2 - 6) = 1035$$

$$\varphi_L(968) = 2975 \text{ cal mol}^{-1}$$

$$\varphi_L(1035) = 2955 \text{ cal mol}^{-1}$$

From equation (8)

$$\Delta H_4 - \Delta H_3 = 13.65 \pm 0.84 \text{ kJ mol}^{-1} \ (3.26 \pm 0.20 \text{ kcal mol}^{-1})$$

c. Evaluation of ΔH_5

From equation (6) and using the above values of ΔH_1, ΔH_2, and $(\Delta H_4 - \Delta H_3)$ we obtain for ΔH_5

$$\Delta H_5 = -340.01 + 259.35 + 13.65$$

$$= -67.01 \pm 4.6 \text{ kJ mol}^{-1} \ (-16.02 \pm 1.1 \text{ kcal mol}^{-1})$$

d. Evaluation of the enthalpy of formation of MoF_5, $\Delta H_f^{\circ}[MoF_5]$

Using equation (7) and the following selected values for enthalpies of formation the enthalpy of formation of MoF_5 can be calculated.

$$\Delta H_f^{\circ}[H_2O(\ell)] = -68.135 \pm .05 \quad \text{kcal mol}^{-1} \qquad [5]$$

$$\Delta H_f^{\circ}[XeO_3(aq)] = 99.94 \pm .24 \quad \text{kcal mol}^{-1} \qquad [8]$$

$$\Delta H_f^{\circ}[HF(aq)] = -80.15 \pm .12 \quad \text{kcal mol}^{-1} \qquad [6]$$

$$\Delta H_f^{\circ}[MoF_6(\ell) = -378.95 \pm .22 \quad \text{kcal mol}^{-1} \qquad [1],[2]$$

$$\Delta H_5 = -16.02 \pm 1.1 \quad \text{kcal mol}^{-1}$$

From these values a value is obtained for the difference in enthalpy of formation of MoF_5 and MoF_6 of

$$\Delta H_f^{\circ}[MoF_5(c)] - \Delta H_f^{\circ}[MoF_6(\ell)] = 189.79 \pm 4.6 \quad \text{kJ mol}^{-1}$$
$$(45.36 \pm 1.1 \quad \text{kcal mol}^{-1})$$

and for the enthalpy of formation of MoF_5 of

$$\Delta H_f^{\circ}[MoF_5(c)] = -1395.74 \pm 4.6 \quad \text{kJ mol}^{-1}$$
$$(-333.59 \pm 1.1 \quad \text{kcal mol}^{-1})$$

In our experiments we have not controlled the stoichiometry to comply exactly with the reaction scheme shown in equations (1) through (5). The effects of differing concentrations of final solutions on the heats of reaction appears to be small compared to other uncertainties of the results and have been neglected in this analysis. In our final data analysis attempts will be made to evaluate the effects of differing concentrations and temperatures between the individual experiments.

5. References

[1] Settle, J. L., Feder, M., Hubbard, W. N., J. Phys. Chem. 5, 1337 (1962).

[2] Parker, V. B., Private communication, Nat. Bur. Std. (U.S.),
     See Ref. [4] for a brief summary.

[3] Wagman, D. D., Evans, W. H., Parker, V. B., Halow, I., Bailey,
     S. M., Schumm, R. H., Nat. Bur. Std. (U.S.) Tech Note 270-4 (1969).

[4] Nuttall, R. L., Churney, K. L., Kilday, M. V., NBS Report 10904,
     Chapt. 1, July 1 (1972).

[5] Wagman, D. D., Evans, W. H., Parker, V. B., Halow, I., Bailey, S. M.,
     Schumm, R. H., Nat. Bur. Std. (U.S.) Tech Note 270-3 (1968).

[6] Wagman, D. D., Private communication, Nat. Bur. Std. (U.S.),
     September, 1973.

[7] O'Hare, P. A. G., Johnson, G. K., Appelman, E. H., J. Inorg.
     Chem. 9, 332 (1970).

[8] Appelman, E. H., and Malm, J. G., J. Am. Chem. Soc. 86, 2141 (1964).

[9] Parker, V. P., Thermal Properties of Aqueous Uni-valent Electrolytes,
     National Standard Reference Data Series--NBS 2 U.S. Govt. Printing
     Office, Washington, DC, 1965.

[10] Krause, R. F., NBS Report 10481, Chapt. 7, (1971).

[11] Prosen, E. J. and Kilday, M. V., J. Res. NBS 77A, 179 (1973).

6. Appendix--Preliminary Experiments

A reaction scheme involving the reaction of $MoF_5(c)$ with an oxidizing agent in aqueous base was investigated because it seemed less likely, a priori, that loss of reactants would occur in basic than in acidic solutions due to the violence of the reaction. Both of the two oxidants considered, $XeO_3(aq)$ and $H_2O_2(aq)$ in 0.3 NaOH, slowly decomposed spontaneously when introduced into the calorimeter, as indicated by a larger than normal drift rate (rate of change of the temperature of the calorimeter with time). The decomposition of $HXeO_4^-$ (the principal species of XeO_3 in our basic solution) before and after its reactions with $MoF_5(c)$ occurred at constant but different rates, as inferred from drift rate data.

The reaction scheme involving basic solutions of $XeO_3(aq)$ was not pursued further since the decomposition implies the presence of xenon in both the VI and VIII oxidation states and $-\Delta G°$ for the change of xenon from the VIII to VI and VI to 0 oxidation states are comparable and large in basic solution (see [8]). Thus, the relative contributions of two oxidation reactions, written below in skeletal form, would have to be evaluated and the heats of formation of both Xe(VI) and Xe(VIII) in basic solution would have to be determined

$$MoF_5(c) + [1/6\,HXeO_4^- + 6\,5/6\,OH^-](soln) = MoO_4^= + 5F^- + 1/6\,Xe(g) + 7/2\,H_2O](soln) \tag{9}$$

$$MoF_5(c) + [1/2\,HXeO_6^{3-} + 6\,OH^-](soln) =$$
$$[MoO_4^= + 5F^- + 1/2\,HXeO_4^- + 3H_2O](soln) \tag{10}$$
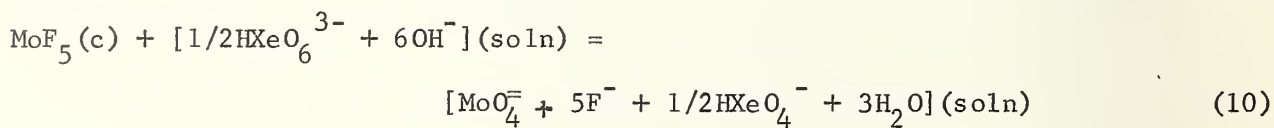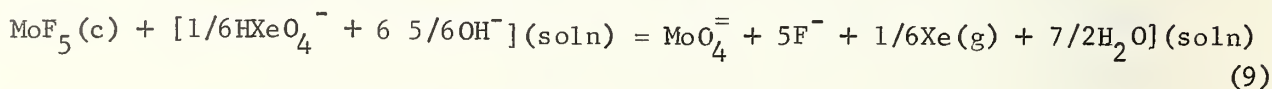
It was of interest to find that our experimental observations in basic solutions of $XeO_3(aq)$ are roughly consistent with those obtained with HF solutions containing $XeO_3(aq)$ presented in the main text. Assuming the rate of decomposition of $HXeO_4^-$ during its reaction with $MoF_5(c)$ was constant and equal to that after the reaction, we obtained a heat of reaction, due to both equations (9) and (10) of -738.9 kJ mol^{-1} (-176.6 kcal mol^{-1}) with an average deviation for five runs of 6.3 kJ mol^{-1} (1.5 kcal mol^{-1}). Assuming the heat of reaction of $MoF_6(\ell)$ with NaOH is independent of the presence of $XeO_3(aq)$ and is equal to the average value of -723 kJ mol^{-1} (172.9 kcal mol^{-1}) obtained in our previous work [4] on $MoF_6(\ell)$, we obtain for various mole fractions, X, of Xenon initially present in the VIII oxidation state:

$$\Delta H_f^\circ[MoF_6(\ell)] - \Delta H_f^\circ[MoF_5(c)] \qquad\qquad X$$

$\qquad$ -197 kJ mol^{-1} (47.1 kcal mol^{-1}) $\quad$ 0.0

$\qquad$ -193 kJ mol^{-1} (46.1 kcal mol^{-1}) $\quad$ 0.03

$\qquad$ -183 kJ mol^{-1} (43.7 kcal mol^{-1}) $\quad$ 0.10

These estimates neglect dilution corrections and are based on an estimated enthalpy of formation of $HXeO_4^-(aq)$ of $+172$ kJ mol^{-1} ($+41$ kcal mol^{-1}) and $\Delta H_f^\circ[HXeO_6^{3-}(aq)] - \Delta H_f^\circ[HXeO_4^-(aq)] \approx +418$ kJ mol^{-1} ($+100$ kcal mol^{-1})[*].

In solutions containing $XeO_3(aq)$ and HF, drift rate data indicated no decomposition of $XeO_3(aq)$ in the reactions involving $MoF_5(c)$. In the case of the $MoF_6(\ell)$ experiments, abnormally large drift rates were observed when the monel holder for the sample bulbs was present in the calorimeter as well as some reaction of the holder with the solution, as indicated by a loss in its weight. Replacement of the monel holder with a platinum holder in the final $MoF_6(\ell)$ experiments eliminated these problems.

------

[*]The maximum uncertainty in $\Delta H_f^\circ[MoF_6(\ell)] - \Delta H_f^\circ[MoF_5(c)]$ is ~ 17 kJ mol^{-1} (4 kcal mol^{-1}).

Table 1. Calorimetric Data for Reaction (1)

Exp. No.	1-1	1-2	1-3	1-4	1-5	Mean
Sample mass, g	.302632	.18911	.17436	.15142	.17922	
Sample mass, moles	.0015850	.0009904	.0009132	.0007930	.0009386	.00010440
Solution composition:						
$6 \cdot n_1$	0.891	0.935	0.963	1.055	1.332	1.035
n_2	16.10	23.43	24.82	28.10	24.33	23.36
$n_3 \times 10^{-3}$	10.255	16.581	18.05	20.85	17.59	16.67
$(\epsilon - 1700)$, $J \cdot K^{-1}$	12.239	8.035	12.231	14.165	9.505	
ΔT_c, K	.314182	.198180	.181220	.157410	.186084	
Q, J	537.954	338.498	310.290	269.827	318.111	
$\overline{T}$, K	298.32	298.22	298.05	298.13	298.06	
$(-\Delta H_1 - 1700)$, $J \cdot g^{-1}$	77.58	89.93	79.60	82.01	74.93	80.81
$-\Delta H_1$, kJ mol^{-1}						340.01
standard deviation, kJ mol^{-1}						1.09
standard deviation of mean, kJ mol^{-1}						.489
$-\Delta H_1$, kcal mol^{-1}						81.26
standard deviation, kcal mol^{-1}						.26
standard deviation of mean, kcal mol^{-1}						.11

Table 2. Calorimetric Data for Reaction (2)

Exp.	Sample g	Mass mmol	Solution Composition			ϵ-1700 JK^{-1}	ΔT_c K	Q J	$\bar{T}$-298.15 K	$-\Delta H_2$	
			$6 \cdot n_1$	n_2	$n_3 \cdot 10^{-3}$					$kJ \cdot mol^{-1}$	$kcal\ mol^{-1}$
2-1	.2327	1.1085	.92	21.4	14.9	11.571	.165315	282.947	-.003	255.25	61.01
2-2	.3733	1.7782	.57	15.6	9.3	11.643	.269408	461.130	.048	259.32	61.99
2-3	.2654	1.2642	.80	17.2	13.0	11.884	.189931	325.140	.010	257.19	61.47
2-4	.1837	0.8751	1.23	21.7	18.9	14.749	.129762	222.508	-.025	254.27	60.77
2-5	.2590	1.2337	.83	18.5	13.3	14.156	.187014	320.571	-.099	259.85	62.10
2-6	.2806	1.3366	.81	16.4	12.3	15.730	.201736	346.125	-.016	258.96	61.89
2-7	.2662	1.2680	.80	19.4	13.0	12.004	.190343	325.868	-.001	256.99	61.42
2-8	.3149	1.5000	.72	10.4	11.0	14.496	.223509	383.205	-.078	255.47	61.06
2-9	.2738	1.3042	.78	16.7	12.7	15.468	.196835	337.664	.004	258.89	61.88
Mean			.83	17.5	13.2					257.35	61.51
Standard Deviation										2.02	.48
Standard Deviation of Mean										.67	.16

Chapter 6

THE VAPOR PRESSURE AT 393 K OF LIQUID MOLYBDENUM PENTAFLUORIDE, MoF_5,

ACCORDING TO PRELIMINARY STATIC-METHOD MEASUREMENTS

by Thomas B. Douglas and Ralph F. Krause, Jr.

Abstract

A new static-pressure method previously developed has reproduced literature vapor-pressure values of I_2 and MoF_6 to within about 1%. In applying the method to MoF_5 (ℓ) in the presence of MoF_6 (g) to prevent disproportionation, it was found necessary to crystallize the MoF_5 to avoid solutions of unknown composition of the components. Preliminary results on the saturated vapor of MoF_5 at 393 K indicate that it contains between 85 and 90 mole % of monomer.

I. Introduction

In the two preceding annual technical reports of this series [1, 2][1] we have reported our successful preparation, purification,

identification, characterization, stabilization, and transpiration

("entrainment") of high-purity molybdenum pentafluoride, MoF_5. Last

year's report [2] gave the results of completed transpiration measure-

ments at three temperatures covering the range 343-383 K, and also

described in detail the design and preliminary testing of a new

_____

[1]Numbers in brackets refer to literature references at the end of this chapter.

static-pressure method, introduced primarily to supplement the transpiration data on MoF_5 with equilibrium data of a different type in order to gain quantitative information on the proportions and thermodynamic properties of the different species $(MoF_5)_n$ known to be present in the vapor. After modifying the apparatus and procedure to mimimize certain systematic errors, they met the original goal of 1% accuracy by reproducing published accurate vapor pressures of I_2 and MoF_6 with approximately this degree of agreement. These successful tests with MoF_6 were made since the last report, so the results are listed in the present report (Section II).

For the past several months the method has been applied to measuring the total pressure of MoF_5[2] vapor, and we had hoped to have by this time a set of final results, at two or more temperatures, on the saturated vapor and perhaps on an unsaturated state as well. Although the work is continuing, this stage has not yet been reached. This is largely so because (as we discovered in our early transpiration work on this substance [1]) a substantial proportion of MoF_6 must be added to prevent appreciable disproportionation of the MoF_5, and consequently the contribution of the MoF_6 to the total pressure must be accurately deducted. In addition, as is well known, static vapor methods (unlike flow methods such as transpiration) deal with such small masses of vapor that wall adsorption of some of it is not negligible and must be accounted for in a reproducible way. Our experience in handling these problems for MoF_5 are discussed later (Section III).

---

[2] Although MoF_5 vapor is a mixture of molecules $(MoF_5)_n$ with different values of $\underline{n}$, it is often convenient to represent the vapor as a whole, or the crystal or liquid, by the simple formula MoF_5.

It was pointed out in last year's report [2] that while a transpiration measurement producing a vapor composed of several molecular species will in some cases give exactly the practical information desired (the mass of material ablated by, or evaporated into, a given flow of gas at a given temperature), neither the apparent vapor pressure nor the apparent heat of vaporization, as derived solely from these data, can be simply related to a single vapor species or to a combination of them. Our early results for the vapor pressure of MoF_5, while imprecise, suggested that the saturated vapor is highly associated and hence is likely to contain several if not many species in major proportions (a conclusion we later revised, as discussed in Section III). For this reason we undertook, concurrently with further experimental work, a mathematical exploration designed to answer several questions as to how many different types of data (transpiration, saturated pressure, unsaturated pressure, etc.) seem worthwhile, how accurate they need to be, and how they can best be applied in interpreting the data thermodynamically. Can one best use a classical thermodynamic approach in which the vapor is simply considered a highly imperfect gas, and if so, what minimum data are required? Or, if one elects to recognize distinct molecular species in the vapor, how many should be taken into account, and with what assumptions such that the data errors are not too greatly magnified when specific-species properties are derived? The significant results of this phase of the investigation are discussed in another report [4].

Unlike substances of universal scientific or practical importance, molybdenum pentafluoride is not of such importance by itself but that such a detailed study on it contrasts sharply with many investigations which apply supposedly well-established methods more or less routinely to a large list of different substances. We feel, however, that much of the experimental and computative information we are acquiring relative to MoF_5 may, rather than lie buried in our notebooks, have equal value when applied to many other substances which behave similarly. Some of the experimental pitfalls of working with unstable substances have not been well recognized, either by the experimenters or by those who review their data. The same can be said for estimating the accuracy of derived properties. If one succeeds in obtaining a reliable and comprehensive set of results on one substance, the results may throw light on the adequacy of competing methods applied to the same substance and properties, as well as contribute to careful planning for future work on other substances. And finally, so little reliable data exist for the lower-valence fluorides of the transition elements that information on one (MoF_5) may contribute in the future to more realistic estimated properties of other members of this class of compounds.

In last year's report [2] we described in detail our develop-
ment of a simple static method to measure small vapor pressures,
especially those of the order of 5 to 30 torr. In principle the
method is briefly as follows. A thermostated vessel of known volume
containing the vapor to be measured is momentarily opened to an
inert gas (argon) which had been at a slightly higher pressure,
measured by a sensitive manometer (di-n-butyl phthalate). The known
volume ratio and the decrease in pressure of the external inert
gas determine the partial pressure of the portion of inert gas mixed
with the vapor, whose degree of association or dissociation has not
appreciably changed because its volume has remained constant. On
the assumption that total-pressure equilibrium has been established,
this partial pressure of inert gas may be subtracted from the final
total pressure to give the desired vapor pressure.

The most important requirement of the apparatus design and
procedure for this type of static-method approach is that virtual
total-pressure equilibrium be attained without appreciable vapor
diffusing out of its vessel and condensing or being absorbed. This
involves compromises, and that they are critical is evidenced by
the fact that we were able to eradicate major vapor-pressure errors
(consistently about 10%) only by making several modifications
described in the earlier report [2]. Thereafter, known pressures
of argon (simulating a vapor) were measured with a mean inaccuracy

of only 0.1%, and the published vapor pressures of iodine at two temperatures were reproduced to about 1%, but the measured values for a vapor pressure of MoF_6 showed a spread of 9% [2].

After several apparatus and procedure improvements, 16 additional measurements of a vapor pressure of MoF_6 (near 236 K, approximately 10 torr) were made. These are individually compared in Table 1 with the vapor-pressure value calculated from the thermodynamic functions of Osborne et al [3], which should be quite accurate; the disagreement averages about 0.7%. (Some of these 16 measurements on MoF_6 were made not to test the method but as auxiliary data needed in measuring MoF_5 as described in Section III.)

The most important improvements in technique preceding the results of Table 1 are as follows. For the seat of the valve through which the inert gas enters the vapor, Teflon replaces metal, making leakage across the closed valve negligible. An Ascarite filter was inserted between this valve and the manometer, thereby preventing in successive valve openings an accummulation outside the vapor vessel of MoF_6 vapor that would react with the manometer oil and affect future measurements appreciably. As in the earlier measurements [2], the valve between inert gas and vapor is still opened usually twice to ensure pressure equilibration, but the optimum time recipe applies to the first opening, viz., taking the accepted manometer reading to 0.01 cm oil (0.008 torr) after opening the

Table 1. <u>Test of the Static-Method: Vapor Pressure</u>
<u>of MoF_6(s) at 236.60 K</u>

(The pressure was observed in an isolated vessel at 298 K after
a period of equilibration with the solid sample near 236.60 K.
This observed vapor pressure was corrected to this nominal temp-
erature, at which the value is 10.61 torr as calculated from the
thermochemical functions of Reference [3]. The experiments are
recorded in chronological order.)

Expt. No.	$(P_{obs}/P_{calc} - 1)100$ %	Expt. No.	$(P_{obs}/P_{calc} - 1)100$ %
1	- 0.9	9	0.0
2	2.6	10	0.1
3	- 0.3	11	0.2
4	- 0.4	12	0.1
5	- 0.1	13	0.3
6	- 0.9	14	- 0.8
7	- 0.4	15	2.2
8	- 0.7	16	1.1

Standard deviation of the mean = 0.25%.

valve for 5 sec and then waiting no more than 1 min. The second
and successive valve openings lead to a drift of values, which
decrease by 0.02 to 0.03 torr for readings near 10 torr after waiting
5 min or more. This decrease is equivalent to an estimate of the
amount of MoF_6 vapor which escapes the vapor vessel during each
valve opening and is adsorbed by the Ascarite.

The MoF_6 was purified as follows. A quantity was distilled
from its supply cylinder, condensed by Dry Ice, pumped for 15 min,
then allowed to warm to room temperature, and finally less than
half distilled to a trap thermostated at about 236 K. The vapor
from this source was then admitted to the previously evacuated vapor
vessel (A or C of Fig. 1, Section III) before beginning static-pressure
measurements an hour later.

Several precautions observed may be mentioned in terms of
their effects on the measured vapor-pressure values reflected in
Table 1. At 236 K the vapor pressure of MoF_6 varies about 10% per
degree, so that the temperature accuracy of the crystalline source
of vapor must be high; in fact, acceptance of the standard thermocouple
tables instead of thermocouple calibration would have made an error
of about 4% in the measured vapor pressure. (A later thermocouple
recalibration indicated a temperature correction equivalent to
0.1% in the MoF_6 vapor pressure.) In a typical experiment measuring
a vapor pressure of about 10 torr, the coefficient of thermal expansion
of the manometric oil and argon is such that an error of 1 deg in

measuring the manometer temperature would itself cause an error of about 0.5% in the measured vapor pressure. One refinement applied was to use a gas-thermometer technique to determine the true average temperature of the part of the inert-gas vessel passing from room temperature to the hot bath containing the vapor vessel; when the latter is at 120°C (the higher temperature used in the work of Section III), it was found that a dependence on spot-temperature measurements would have introduced an error of about 0.1% in the vapor pressure. An error of similar magnitude would have resulted if the expansion of the glass vessels from room temperature to 120°C had been ignored.

III. Preliminary: Static-Method Vapor-Pressure Measurements on MoF_5 (ℓ) at 392.6 K

The test measurements on "known" cases outlined in the preceding section satisfied us that our original goal of developing a static method for measuring simple vapor pressures in the range of 5 to 30 torr to an accuracy of about 1% had been met. We then proceeded to apply the method to measuring vapor pressures of liquid MoF_5. Besides the lack of known values for comparison, this substance presents the complication of a tendency to disproportionate which, our transpiration work [1, 2] had showed, can be satisfactorily suppressed only by having present a considerable partial pressure of MoF_6 vapor which must be determined independently and subtracted from the total pressure of the vapor mixture to give the equilibrium pressure of the MoF_5 vapor.

Our first series of measurements on MoF_5 were made using the earlier version of the apparatus [2] in the following way. A desired amount of MoF_5 (15 to 30 times enough to saturate the vapor space at the final temperature) was transpired into the "vapor vessel," which was near room temperature (where the vapor pressure of MoF_5 is of the order of 0.01 torr). Before each experiment the vessel containing the supercooled MoF_5 liquid was opened to vacuum (near 10^{-5} torr at the pump) for over an hour. The vessel and the supercooled MoF_5 (liquid) sample were subsequently thermostated at 311 K, and then supposedly equilibrated with MoF_6 vapor at a pressure (50 to 100% of that expected for MoF_5 vapor) which was controlled by and accurately known [3] because of its contact with the purified crystal thermostated at a suitable low temperature. The vapor vessel was then isolated by closing the valve, heated to and thermally equilibrated at the final temperature (393 or 408 K). From the subsequently determined total pressure was subtracted the partial pressure at this temperature of the number of moles of MoF_6 vapor present at the lower temperature.

The precision of our earliest vapor-pressure values for MoF_5 (9 experiments near, and corrected to, 393 K; and 4 experiments near, and corrected to, 408 K) was distinctly disappointing. These values showed, however, some indication of converging toward a value which, compared with the transpiration value at the same temperature, indicated an average degree of association near 2. This led to the tentative conclusion that saturated MoF_5 vapor (at these temperatures) must

99

be composed of major proportions of several species [several values of $\underline{n}$ for $(MoF_5)_n$], and instigated the examination of the several alternative ways of handling the thermodynamics of such a vapor that are described in another report [4].

In attempting to explain the poor precision and to uncover consistent errors that improved precision might hide, rough calculations suggested that the following systematic errors in the procedure thus far for MoF_5 may have been too large to dismiss without experimental tests and, if necessary, application of suitable corrections:

(a) The fluoride vapors may have been reacting chemically with the hot Pyrex walls. (In subsequent tests in which the valve to the vapor vessel at 393 K was opened at hourly intervals, the total number of gaseous moles thereby registered remained so constant as to indicate that the walls were either inert or had become so.)

(b) Wall adsorption of MoF_5 should not be a problem, owing to the excess of the liquid phase. But in heating the isolated vessel containing MoF_6 by almost 100 deg, the decrease in wall adsorption of the MoF_6 may be too large to ignore. (In four separate special experiments a glass vessel at 311 K was filled with MoF_6 vapor to a pressure of 6.606 torr, then closed and heated to 393 K. In each of the last three experiments the subsequently measured pressure at 393 K exceeded 6.606(393/311) by 1.0%. The surface-to-volume ratio of the vessel was nominally 1.6 cm^{-1}, but believed to be actually greater by a factor of 3. A treatment using this information

and the Brunauer-Emmett-Teller adsorption equation indicated a decrease in adsorption equivalent to 0.07 torr of MoF_6 at the higher temperature for all pressures from 1 to 10 torr, and this small correction was applied in all future measurements.)

(c) The amount of MoF_6 dissolving in the liquid MoF_5 may have been too large to ignore. (A simple ideal-solution estimation indicated a solubility of the order of 0.001 mol fraction--too small to lower the partial pressure of MoF_5 by an amount outside the accuracy of the method; but enough to increase the pressure of MoF_6 by as much as 23% when the supercooled MoF_5 liquid was heated from 311 to 393 K.)

(d) The liquid MoF_5 may have contained enough lower subfluoride (such as MoF_4) to destroy an appreciable fraction of the MoF_6 in a reversal of the disproportionation. (Even though the supercooled MoF_5 liquid was supposedly equilibrated in each experiment of the first series, this treatment may not have been effective owing to the lack of stirring. Error (d) existed in the transpiration measurements on MoF_5 [1, 2] except that in that case there was no necessity of accounting for the total MoF_6 introduced, and the large excess used was sufficient to purify increasingly the MoF_5 liquid along its length in the transpiration tube. However, in a static method an impurity of only 0.15 mol % [1] in the MoF_5 could under certain circumstances lead to a fatal error. Error (d) is like Error (c) above in being worse, but of opposite sign, for larger liquid

samples. Before we were aware of the importance of Error (d), we had hoped to make Error (c) negligible and have a better account of the MoF_6. In a second series of experiments, we used a much smaller liquid sample, 3 times enough to saturate the vapor space at the final temperature of 393 K; and expanded at 298 K, in contrast to the earlier equilibration at 311 K, a predetermined quantity of MoF_6 vapor into the vapor vessel containing the supercooled MoF_5 liquid. We seemed to find, however, that resorting to a much smaller liquid sample tends to introduce even greater errors, among them in this case the failure to equilibrate the MoF_5 sample beforehand with MoF_6.)

To avoid Errors (c) and (d) we revised the procedure as applied to MoF_5 so as to be able to subtract from the total pressure not the original but the final amount of MoF_6, and the apparatus modified accordingly is diagrammed in Fig. 1. (The volume of each vessel A, B, and C is about 80 cm^3.) Before the first subsequent run, the MoF_5 sample (about 10 times the amount needed to fill Vessels A, B, and C with saturated vapor at 393 K) was entrained into B while Vessels A and C were detached. After installing, pretreating, and evacuating A and C, vessel B at room temperature was opened to vacuum for about an hour. (In this series a vacuum gauge which was installed near the vessels served as an evacuation test of 10^{-5} torr after the pump was isolated.)

STATIC PRESSURE APPARATUS

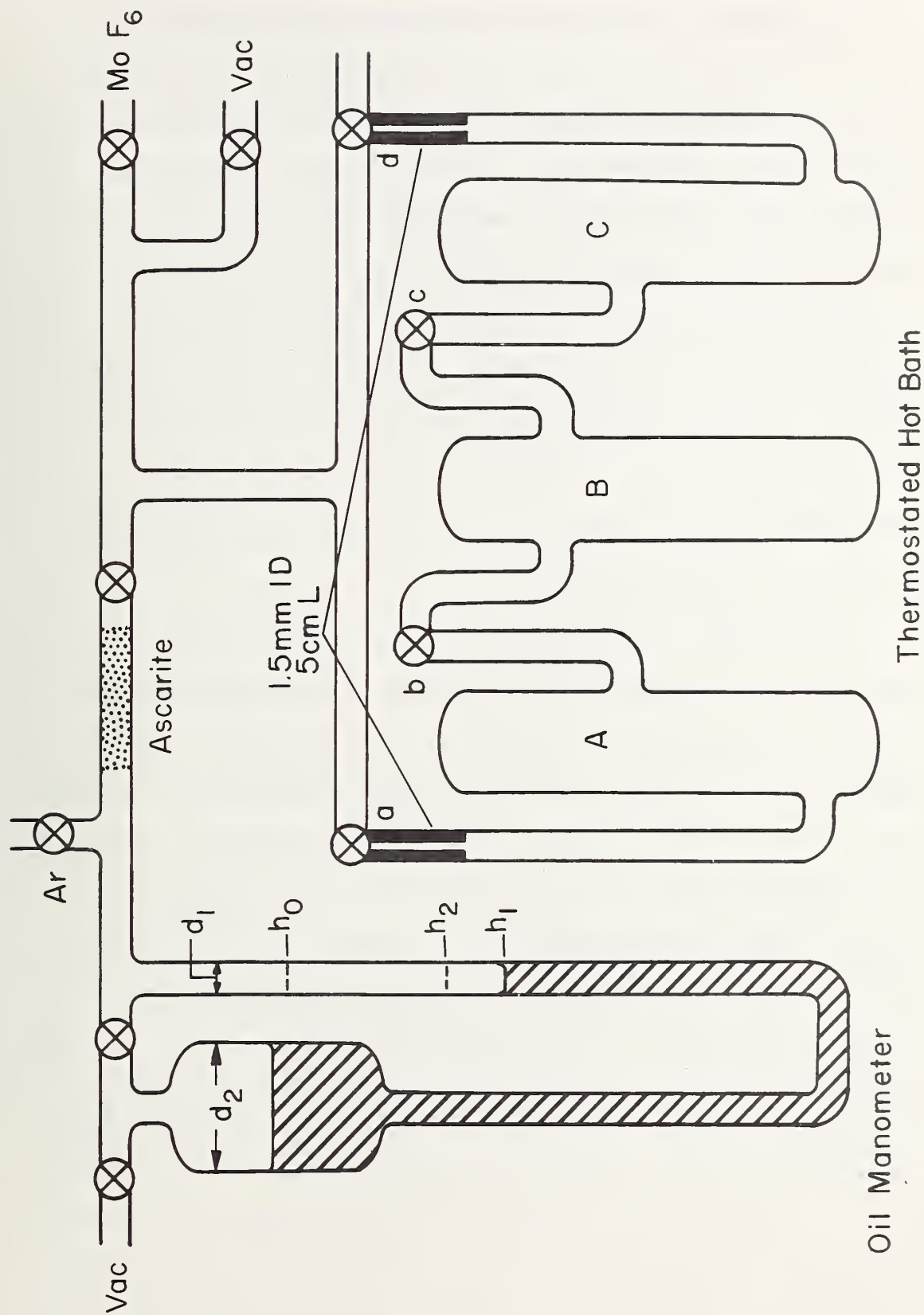Mo F$_6$

Vac

Ar

Vac

Ascarite

1.5mm ID
5cm L

d_1

h_0

h_2

h_1

d_2

a

b

c

d

A

B

C

Thermostated Hot Bath

Oil Manometer

FIGURE 1.   Revised static-method apparatus used to measure the vapor pressure of MoF$_5$ (schematic).

In contrast to the two earlier series, vacuum pumping was applied at 298 K only to crystalline, not supercooled liquid, MoF_5. A suitable pressure of MoF_6 was then equilibrated for about an hour with the crystalline MoF_5 at 298 K. As shown later, this suitable pressure was several times smaller than a critical pressure needed to support a MoF_6 - containing liquid in equilibrium with crystalline MoF_5. Valves a and d were then closed (but b and c left open--they have no capillaries, in order to promote diffusion of MoF_5 vapor from B into A and C), and the bath was then heated during the next hour to a nominal temperature of 393 K and thermostated at that temperature for the next hour before beginning static-pressure measurements.

After closing Valves b and c, the total pressure in A or C-- or, separately, in both--was then measured in the manner previously described, by admitting argon through a or d respectively. The bath was then cooled (45 min) to a nominal temperature of 298 K, and after another hour the total pressure (now due almost entirely to MoF_6) was measured by the standard procedure in A or C or, separately, in both. When this measurement was on a vessel on which a measurement had previously been made at the higher temperature, it was necessary to subtract off the usually small contribution of the argon that had previously entered before multiplying the observed MoF_6 pressure by the exact temperature ratio (nominally, 393/298), adding

the adsorption correction previously discussed (0.07 torr), and then subtracting this corrected value from the total pressure measured at 393 K, to get the net vapor pressure of the MoF_5 at this temperature.

One further precaution observed in the above procedure should be mentioned. On cooling A and C to 298 K, the formerly saturated MoF_5 vapor condenses and is so viscous that it normally supercools and remains liquid, and a simple ideal-solution calculation suggests that this liquid would be sufficient in amount to dissolve about 2% of the MoF_6. However, the melting point of MoF_5 is about 319 K [1], and another ideal-solution calculation showed that at 298 K pure crystalline MoF_5 can exist in equilibrium with MoF_6-containing liquid only if the ambient pressure of MoF_6 exceeds about 100 torr, which is many times that in our work. Consequently, the crystallization of the condensed MoF_5 in A or C was always induced (by seeding with a Dry-Ice slush applied externally over about 1 cm^2) before undertaking to measure the MoF_6 pressure.

The essential results of all measurements made by the above revised procedure up to the time of this writing are given in Table 2. The so-called "experiments" (or runs) are numbered and enumerated (one per line) in chronological order, as chronological trends appear to be very significant. (The same charge of liquid MoF_5 was used for all eight experiments, and there is reason to suppose that the purities of the sample portions in the three vessels changed progressively, if at all, during the course of these experiments.) The

Table 2. Static-Method Measurements of the

Vapor Pressure of $MoF_5(\ell)$ at 392.6 K

(The data of an experiment are used to calculate the vapor pressure in as many as 3 alternate ways. All pressures are corrected to 392.6 K as explained in the text, p_5 represents $\Sigma P_n[(MoF_5)_n(g)]$ in torr, and p_6 represents $P[MoF_6(g)]$ in torr. 1 torr = $101,325/760$ N/m^2.)

1	2	3	4	5	6	7	8
Expt. No.[e]	$p_5 + p_6$ (obs)[a]	p_6 (obs)[b]			p_5 (calc), using:		
		initial	final[c]		initial	final	
		A and C	A	C	A and C	A	C
1	7.74	--	1.70[d]	1.74	--	6.04	6.00
2	16.26	9.36	3.98	5.60[d]	6.90	12.28	10.66
3	19.77	9.42	--	7.57	10.35	--	12.20
4	21.29	9.40	7.26	9.15	11.89	14.03	12.14
5	21.27	9.27	7.96	9.29	12.00	13.31	11.98
6	20.67	9.24	8.36[d]	9.51	11.43	12.31	11.16
7	20.73	9.26	8.76[d]	9.55	11.47	11.97	11.18
8	12.87	--	1.41	--	--	11.46	--
Mean (Expt. 4-7)					11.70	12.90	11.62

[a]Measured in vessel A for experiments 2, 4, 5, and 8 and in vessel C for experiments 1, 3, 4, 5, 6, and 7. Differences of 0.2 and 0.3% were observed for experiments 4 and 5 respectively.

[b]Measured same day as ($p_5 + p_6$) for experiments 6, 7, and 8, but the next day for the other experiments.

[c]Applied correction for decrease of wall adsorption (but no correction for initial values, in which decrease of wall adsorption was assumed to cancel increase of MoF_6 solution in $MoF_5(\ell)$).

[d]No prior introduction of argon, which was corrected for in all other final p_6 values.

[e]Not related to the Experiment Nos. of Table 1.

partial pressures of the individual vapor species are assumed

additive, with p_5 symbolizing the sum of the $(MoF_5)_n$ partial

pressures ("vapor pressure" of MoF_5 (ℓ)) and p_6 symbolizing the

pressure or partial pressure of MoF_6, which is known not to

associate (except in the dispersion sense, which can be ignored

here). The higher temperature actually varied from 392.38 to

392.64 K, but for comparison purposes all the values have been

corrected to 392.6 K by assuming that p_6 is proportional to the

absolute temperature, and that near 392.6 K, p_5 increases by 5.8%

per deg [2].

The total pressure $(p_5 + p_6)$ was measured sometimes in Vessel

A, sometimes in Vessel C, and in two experiments in both A and C

with only about 0.05 torr disagreement, so that a single value is

listed for each experiment. On the other hand we may consider that

we have for each (complete) experiment three generally different

values for p_6 (Columns 3-5), which when subtracted from Column 2

give three alternate values for p_5 (Columns 6-8, respectively).

(Column 3 was derived from the vapor pressure of MoF_6 at its condensed

source [3]; Columns 4 and 5 are as measured in the foregoing

procedure.)

Experiments 1 and 8, with no MoF_6 deliberately introduced

(Column 3), were undertaken to allow an estimate of the residual

disproportionation in the other experiments, and will be discussed

later. Let us direct our attention first to Experiments 2-7. According

to the earlier discussion, the use of either Column 4 or 5 should

obviate error arising from failure to account for whatever MoF_6

is absorbed by the bulk of liquid MoF_5 (in Vessel B), and indeed each of these two columns is seen to increase sharply with time and in the later experiments approach the neighborhood of the respective initial "pressures" of MoF_6 shown in Column 3. Yet the corresponding Columns 7 and 8 are not constant, but (except for some unexplained irregularity at first) drift downward with time, and may be approaching, at different rates but rather asymptotically, approximately the same value. Although other factors, such as possibly a more volatile impurity at first, may be involved, we are inclined to feel that the downward drifts of Columns 7 and 8 reflect persistent but declining losses of MoF_6 vapor (different in A than in C), through reaction with the walls or impurity in the condensed MoF_5, that eventually would have become completed.

In this connection it is significant that the vapor-pressure values of Column 6, which were calculated in the earlier manner, settle down after Experiment 3 to the neighborhood of the "asymptotic" limits of Columns 7 and 8. This seems not surprising if we assume that by the later experiments the bulk of liquid MoF_5 has had its postulated disproportionation reversed to the point where in each succeeding experiment this liquid absorbs MoF_6 at 393 K only through solubility, an effect estimated to be perhaps 1 to 2% and offset by a wall desorption (deliberately uncorrected for in Columns 3 and 6) of similar magnitude but opposite sign.

In the light of the above discussion, Experiment 1 is premature for estimating the disproportionation equilibrium, but Experiment 8 was used for this purpose. Assuming the disproportionation products of MoF_5 to be MoF_6 and MoF_4 (the latter is uncertain, but still lower fluorides such as MoF_3 would lead to even less serious error), the 1.41 torr of MoF_6 measured in Experiment 8 determines approximately the concentration of MoF_4 dissolved in our particular amount of liquid MoF_5, and suggests for our case a mole fraction of about 0.01 for the MoF_4 in the liquid and hence a vapor-pressure of MoF_5 (MoF_4 is much less volatile) too low by 1% owing to this cause. However, the same equilibrium constant indicates that in Experiments 2-7, where the pressure of MoF_6 is about 5 times as great, the mol fraction of MoF_4 would be only about 0.002 (0.2% error).

Finally, it is of interest to examine what our data so far indicate for the composition of saturated $(MoF_5)_n$ vapor at 392.6 K. The two-constant "best" empirical equation fitting our transpiration data at 343, 363, and 383 K [2] gives $\Sigma nP_n = 13.3$ torr at 392.6 K, and we can tentatively take $\Sigma P_n = 11.7$ torr from Table 2. If we assume only monomer and dimer, these two values give $P_1 = 10.1$ torr, $P_2 = 1.6$ torr, and mole fractions of 0.86 and 0.14, respectively. On the other hand, if we follow the treatment of Section II 2 of a related chapter in another report [4] by assuming values of n from 1 to ∞ but a constant ratio P_{n+1}/P_n, we get $P_1 = 10.3$ torr, $P_2 = 1.2$ torr, $P_3 = 0.15$ torr, ..., and mole fractions of 0.88, 0.11, 0.015, ...,

respectively (with correspondingly smaller proportions of the higher species). The two treatments thus indicate approximately the same abundances of the monomer and the dimer.

We hope to have the opportunity to make some additional static-pressure measurements of the vapor pressure of MoF_5 at 392.6 K in order to test the validity of the trends appearing in Table 2, and to extend the measurements to another temperature sufficiently different as to enable us to determine the heats of the reactions involving $MoF_5(\ell)$, $MoF_5(g)$, and/or $(MoF_5)_2(g)$.

IV. References

[1]   R. F. Krause, Jr., AFOSR Scientific Report AFOSR-TR-71-2584 (NBS Report 10481), National Bureau of Standards, Washington, D. C. 20234, July 1971, Chapter 7 (pp. 97-109).

[2]   T. B. Douglas and R. F. Krause, Jr., AFOSR Scientific Report AFOSR-TR-72-2004 (NBS Report 10904), National Bureau of Standards, Washington, D. C. 20234, July 1972, Chapter 2 (pp. 29-48).

[3]   D. W. Osborne, F. Schreiner, J. G. Malm, H. Selig, and L. Rochester, J. Chem. Phys. 44, 2802-2809 (1966).

[4]   T. B. Douglas and R. F. Krause, Jr., "Alternative Procedures in Interpreting Equilibrium Data on Partially Associated Vapors," Chapter 4 of Report NBSIR 73-280, National Bureau of Standards, Washington, D. C. 20234 (AFOSR-ISSA-72-0007), 1 January 1973.

DOCUMENT CONTROL DATA - R & D

(Security classification of title, body of abstract and indexing annotation must be entered when the overall report is classified)

1 ORIGINATING ACTIVITY (Corporate author)	2a. REPORT SECURITY CLASSIFICATION
NATIONAL BUREAU OF STANDARDS DEPARTMENT OF COMMERCE WASHINGTON, D. C. 20234	UNCLASSIFIED
	2b. GROUP

3 REPORT TITLE

THERMODYNAMICS OF CHEMICAL SPECIES IMPORTANT TO ROCKET TECHNOLOGY

4. DESCRIPTIVE NOTES *(Type of report and inclusive dates)*

Scientific   Final

5. AUTHOR(S) *(First name, middle initial, last name)*

Thomas B. Douglas
Charles W. Beckett

6 REPORT DATE	7a. TOTAL NO OF PAGES	7b. NO. OF REFS
1 July 1973	120	56

8a. CONTRACT OR GRANT NO	9a. ORIGINATOR'S REPORT NUMBER(S)
AFOSR-ISSA-73-0001	
b. PROJECT NO 9750-01	NBSIR 73-281
c. 61102F	9b. OTHER REPORT NO(S) *(Any other numbers that may be assigned this report)*
d. 681308	AFOSR-TR-74-0063

10 DISTRIBUTION STATEMENT

Approved for public release; distribution unlimited.

11 SUPPLEMENTARY NOTES	12 SPONSORING MILITARY ACTIVITY
TECH, OTHER	AF Office of Scientific Research/NC 1400 Wilson Boulevard Arlington, Virginia 22209

13 ABSTRACT

Using a subsecond-duration transient technique, the specific heat, electrical resistivity, and hemispherical total emittance were simultaneously measured 1500-2800 K for iron and the alloy 80Nb-10Ta-10W (estimated uncertainties: 3%, 0.5-1%, and 3% for the respective properties). Comparisons are made with generalized approximations. At the gamma-to-delta transformation of iron (about 1680 K), the temperature, heat of transformation, specific heat, spectral emittance, and electrical resistivity were measured, thereby demonstrating the feasibility of the technique for solid-solid transformations. Two other alloys were likewise measured. Solution calorimetry involving several thermochemical steps (including oxidation by XeO_3 in aqueous HF) gave the standard heat of formation of $MoF_5(c)$. A new static vapor-pressure method, after verification to 1% by I_2 and MoF_6, and after modifications to deal with the necessarily added MoF_6, gave the vapor pressure of MoF_5 at 393 K and indicated (using also earlier NBS transpiration data) 85-90 mole % of monomer in the saturated vapor.

DD FORM 1473
1 NOV 65

14 KEY WORDS	LINK A		LINK B		LINK C	
	ROLE	WT	ROLE	WT	ROLE	WT
ELECTRICAL RESISTIVITY						
IRON						
MOLYBDENUM PENTAFLUORIDE						
PARTLY ASSOCIATED VAPORS						
SOLID-STATE TRANSFORMATIONS						
SOLUTION CALORIMETRY						
SPECIFIC HEAT						
SPECTRAL EMITTANCE						
VAPOR PRESSURE						
TRANSITION ALLOYS						